© 2015. Published by The Company of Biologists Ltd | Development (2015) 142, 497-509 doi:10.1242/dev.115576

RESEARCH ARTICLE

β-catenin-dependent transcription is central to Bmp-mediated formation of venous vessels

Takeru Kashiwada[1,2], Shigetomo Fukuhara[1,*], Kenta Terai[3], Toru Tanaka[1,2], Yuki Wakayama[1], Koji Ando[1], Hiroyuki Nakajima[1], Hajime Fukui[1], Shinya Yuge[1], Yoshinobu Saito[2], Akihiko Gemma[2] and Naoki Mochizuki[1,4,*]

ABSTRACT

β-catenin regulates the transcription of genes involved in diverse biological processes, including embryogenesis, tissue homeostasis and regeneration. Endothelial cell (EC)-specific gene-targeting analyses in mice have revealed that β-catenin is required for vascular development. However, the precise function of β-catenin-mediated gene regulation in vascular development is not well understood, since β-catenin regulates not only gene expression but also the formation of cell-cell junctions. To address this question, we have developed a novel transgenic zebrafish line that allows the visualization of β-catenin transcriptional activity specifically in ECs and discovered that β-catenin-dependent transcription is central to the bone morphogenetic protein (Bmp)-mediated formation of venous vessels. During caudal vein (CV) formation, Bmp induces the expression of *aggf1*, a putative causative gene for Klippel–Trenaunay syndrome, which is characterized by venous malformation and hypertrophy of bones and soft tissues. Subsequently, Aggf1 potentiates β-catenin transcriptional activity by acting as a transcriptional co-factor, suggesting that Bmp evokes β-catenin-mediated gene expression through Aggf1 expression. Bmp-mediated activation of β-catenin induces the expression of Nr2f2 (also known as Coup-TFII), a member of the nuclear receptor superfamily, to promote the differentiation of venous ECs, thereby contributing to CV formation. Furthermore, β-catenin stimulated by Bmp promotes the survival of venous ECs, but not that of arterial ECs. Collectively, these results indicate that Bmp-induced activation of β-catenin through Aggf1 regulates CV development by promoting the Nr2f2-dependent differentiation of venous ECs and their survival. This study demonstrates, for the first time, a crucial role of β-catenin-mediated gene expression in the development of venous vessels.

KEY WORDS: β-catenin, Venous vessel development, Bmp, Aggf1, Nr2f2, Zebrafish

INTRODUCTION

β-catenin is a transcriptional regulator that mainly acts downstream of Wnt signaling and mediates diverse cellular functions including proliferation, survival and fate determination during embryogenesis, tissue homeostasis and regeneration (Angers and Moon, 2009; Clevers, 2006; Logan and Nusse, 2004; MacDonald et al., 2009). In the absence of Wnt signaling, cytosolic β-catenin is phosphorylated by a destruction complex composed of axin, adenomatous polyposis coli and glycogen synthase kinase 3β, which leads to degradation of β-catenin via the ubiquitin-proteasome pathway. Wnt inhibits the activity of this destruction complex, resulting in the stabilization and nuclear translocation of β-catenin. In the nucleus, β-catenin associates with the T-cell factor (Tcf)/lymphoid enhancer factor family of transcription factors, thereby inducing the transcription of target genes. In addition, β-catenin regulates cell-cell adhesions by linking cadherin molecules to the actin cytoskeleton via α-catenin (Dejana et al., 2008).

β-catenin has been implicated in many aspects of vascular development and maintenance. Mice deficient in β-catenin in endothelial cells (ECs) exhibit embryonic lethality due to defective vascular patterning, increased vascular fragility and impaired cardiac valve formation (Cattelino et al., 2003; Liebner et al., 2004). The phenotypes caused by EC β-catenin deficiency are thought to be attributable to not only the impairment of EC junctions but also the loss of the Wnt/β-catenin pathway. Therefore, it is important to explore the involvement of β-catenin-dependent transcriptional regulation in vascular development by clearly distinguishing the role of β-catenin in gene regulation from that in cell-cell adhesion.

The Wnt/β-catenin pathway promotes sprouting angiogenesis in the central nervous system and controls blood-brain barrier development (Daneman et al., 2009; Liebner et al., 2008; Stenman et al., 2008). Wnt/β-catenin signaling also cooperates with the Notch pathway in vascular development. Notch-regulated ankyrin repeat protein acts as a molecular link between the Notch and Wnt/β-catenin pathways in ECs (Phng et al., 2009). Furthermore, the Wnt/β-catenin pathway potentiates Notch signaling by inducing the expression of Dll4, which modulates vascular remodeling and arterial EC specification during early development (Corada et al., 2010; Yamamizu et al., 2010; Zhang et al., 2011). However, a recent report indicated that Dll4 expression in ECs and subsequent arterial specification are not mediated by the Wnt/β-catenin pathway *in vivo* (Wythe et al., 2013). Therefore, the role of β-catenin-dependent transcription in vascular development has yet to be elucidated.

It is widely accepted that the optimal way to analyze the role of β-catenin-dependent transcription in ECs during vascular development is to directly visualize its activity exclusively in ECs *in vivo*. To date, several transgenic (Tg) murine models have been developed to detect the *in vivo* transcriptional activity of β-catenin (DasGupta and Fuchs, 1999; Maretto et al., 2003). However, these reporter mice do not faithfully reproduce endogenous β-catenin transcriptional activity (Ahrens et al., 2011; Al Alam et al., 2011). In addition, several zebrafish reporter lines that express fluorescent proteins under the control of a β-catenin/Tcf-responsive promoter have been generated (Dorsky et al., 2002; Moro et al., 2012;

[1]Department of Cell Biology, National Cerebral and Cardiovascular Center Research Institute, Fujishirodai 5-7-1, Suita, Osaka 565-8565, Japan. [2]Department of Pulmonary Medicine and Oncology, Graduate School of Medicine, Nippon Medical School, Tokyo 113-8603, Japan. [3]Laboratory of Function and Morphology, Institute of Molecular and Cellular Biosciences, The University of Tokyo, Tokyo 113-0032, Japan. [4]JST-CREST, National Cerebral and Cardiovascular Center Research Institute, Fujishirodai 5-7-1, Suita, Osaka 565-8565, Japan.

*Authors for correspondence (fuku@ncvc.go.jp; nmochizu@ncvc.go.jp)

Received 20 July 2014; Accepted 4 December 2014

Development (2015) 142, 497-509 doi:10.1242/dev.115576

Shimizu et al., 2012). However, they might not be suitable for studying β-catenin-dependent transcription in ECs, since the reporter gene expression is not restricted to the vasculature.

We have developed a novel Tg zebrafish line that allows us to visualize the β-catenin transcriptional activity in ECs, revealing β-catenin-mediated transcription in specific parts of the vasculature, including the caudal veins (CVs), in developing embryos. During CV formation, bone morphogenetic protein (Bmp) induces the expression of Angiogenic factor with G patch and FHA domains 1 (Aggf1), which in turn stimulates β-catenin transcriptional activity. Subsequently, activated β-catenin mediates CV formation by promoting venous EC differentiation through the expression of Nuclear receptor subfamily 2, group F, member 2 (Nr2f2, also known as Coup-TFII) and by maintaining their survival.

RESULTS

Development of an EC-specific β-catenin reporter zebrafish line

To monitor the transcriptional activity of β-catenin, we constructed a plasmid encoding a β-catenin-dependent Gal4 driver (Gal4db-TΔC) that contains the β-catenin-binding domain of Tcf4 fused to the DNA-binding domain of Gal4. To ascertain whether this driver can be stimulated by β-catenin, HEK 293T cells were transfected with plasmid encoding Gal4db-TΔC and an upstream activation signal (UAS)-luciferase reporter together with a β-catenin-expressing plasmid. β-catenin overexpression induced luciferase expression in the cells expressing Gal4db-TΔC, but not in those expressing the mutant form Gal4db-TΔC (D16A), which lacks β-catenin binding capacity (supplementary material Fig. S1A). Treatment with BIO, a glycogen synthase kinase 3 inhibitor, potentiated the Gal4db-TΔC-driven reporter gene expression (supplementary material Fig. S1B). These results indicate that reporter gene expression driven by the β-catenin-dependent Gal4 driver reflects the transcriptional activity of β-catenin.

To visualize β-catenin transcriptional activity in ECs, we developed a Tg zebrafish line that expresses a fusion protein containing Gal4db-TΔC, 2A peptide and mCherry (Gal4db-TΔC-2A-mC) under the control of the *fli1* promoter. Then, we crossed it with *UAS:GFP* reporter fish to generate the *Tg(fli1:Gal4db-TΔC-2A-mC);(UAS:GFP)* line, which we refer to as EC-specific β-catenin reporter fish (Fig. 1A). In EC-specific β-catenin reporter fish with the *Tg(fli1:Myr-mC)* background, GFP was observed in particular regions of ECs together with mCherry fluorescence (Fig. 1B). However, most of the mCherry-marked blood vessels emitted GFP fluorescence upon heat shock promoter-mediated overexpression of Wnt3a, an activator of canonical β-catenin signaling (Fig. 1B). Furthermore, in BIO-treated embryos most of the ECs exhibited GFP, whereas GFP expression was significantly suppressed by treatment with IWR-1, which promotes β-catenin degradation by stabilizing axin (Chen et al., 2009) (Fig. 1C,D; supplementary material Fig. S1C). These results indicate that the GFP in our EC-specific β-catenin reporter fish line reflects the transcriptional activity of β-catenin in ECs.

Visualization of β-catenin transcriptional activity in ECs during vascular development

We investigated how β-catenin-mediated transcription in ECs is spatiotemporally controlled during vascular development by analyzing our EC-specific β-catenin reporter fish. The GFP signal was first detected in the cranial vessels at 24 h post-fertilization (hpf), and reached a maximum at 36 hpf (Fig. 1E). Consistent with the role of endocardial Wnt/β-catenin signaling in cardiac valve formation (Hurlstone et al., 2003), the GFP signal was detected in endocardial ECs at 48 hpf (Fig. 1E). The ECs in the common cardinal veins also expressed GFP at 36 hpf (Fig. 1E). Furthermore, GFP was observed in the caudal vessels starting at 26 hpf, but this fluorescence was confined to the CV at 48 hpf (Fig. 1E). These observations imply that β-catenin plays a significant role in vascular development.

Crucial role of β-catenin-dependent transcription in CV formation

CV formation involves venous fate specification/differentiation, venous sprouting and remodeling, making it suitable for studying venous vessel formation (Choi et al., 2011; Kim et al., 2012; Wiley et al., 2011). To address the role of β-catenin in CV formation, we first analyzed CV formation during development (supplementary material Fig. S2). The CV primordia initially formed just beneath the caudal artery (CA) at 24 hpf, as previously reported (Choi et al., 2011). Then, the ECs sprouted from the CV primordia to migrate ventrally at 28 hpf, and formed a CV plexus (CVP) at 36 hpf. At 48 hpf, the ECs in the ventral region of the plexus underwent remodeling to establish the CV, while some ECs in the dorsal part of the plexus migrated dorsally to form secondary sprouts. During the next few days of development, the CVP relocated ventrally and fused to the CV, while some ECs in the plexus regressed during this process.

To investigate when and where β-catenin-dependent transcription occurs during CV formation, we performed time-lapse imaging of EC-specific β-catenin reporter fish embryos. GFP expression was dramatically induced in the ECs that had just sprouted from the CV primordia (Fig. 2A; supplementary material Movie 1). These GFP-positive ECs migrated ventrally, became located in the ventral part of the CVP, and finally formed the CV (Fig. 2A,B; supplementary material Movie 1). However, GFP fluorescence gradually decreased once the CV had formed, suggesting a transient role of β-catenin-mediated gene expression in CV formation.

To address this hypothesis, we analyzed *Tg(fli1:Gal4FF);(fli1:Myr-mC)* embryos injected with a *UAS:axin,NLS-GFP* Tol2 plasmid, which drives the expression of axin and NLS-GFP simultaneously in ECs, and found that axin-overexpressing ECs, in which β-catenin degradation was facilitated, failed to contribute to CV formation (supplementary material Fig. S2B,C). Furthermore, we inhibited β-catenin/Tcf-dependent transcription in ECs by generating *Tg(fli1:Gal4FF);(UAS:RFP);(UAS:TΔN-GFP)* fish embryos. Expression of dominant-negative Tcf (TΔN-GFP) in these ECs resulted in impairment of CV formation, but did not affect CA formation (Fig. 2C,D). These results indicate the essential role of β-catenin-dependent transcription in CV development but not in CA formation. During CV formation, nuclear fragmentation occurred in the TΔN-GFP-expressing ECs, but not in those expressing NLS-GFP (Fig. 2E,F; supplementary material Movie 2). Among the TΔN-GFP-expressing ECs, most of the cells undergoing nuclear fragmentation were found in the CVP, although a small number of the ECs in the CA also underwent nuclear fragmentation (Fig. 2E,F; supplementary material Movie 2). In addition, TUNEL analyses revealed that TΔN-GFP expression induced EC apoptosis in the CVP, but not in the CA (Fig. 2G,H).

Collectively, these findings indicate that β-catenin-dependent transcription regulates CV formation by promoting the survival of venous ECs, whereas it is not necessary for the survival of arterial ECs.

Activation of β-catenin-dependent transcription by Bmp during CV formation

We next sought to identify the upstream signaling molecules that stimulate β-catenin transcriptional activity during CV formation,

Development (2015) 142, 497-509 doi:10.1242/dev.115576

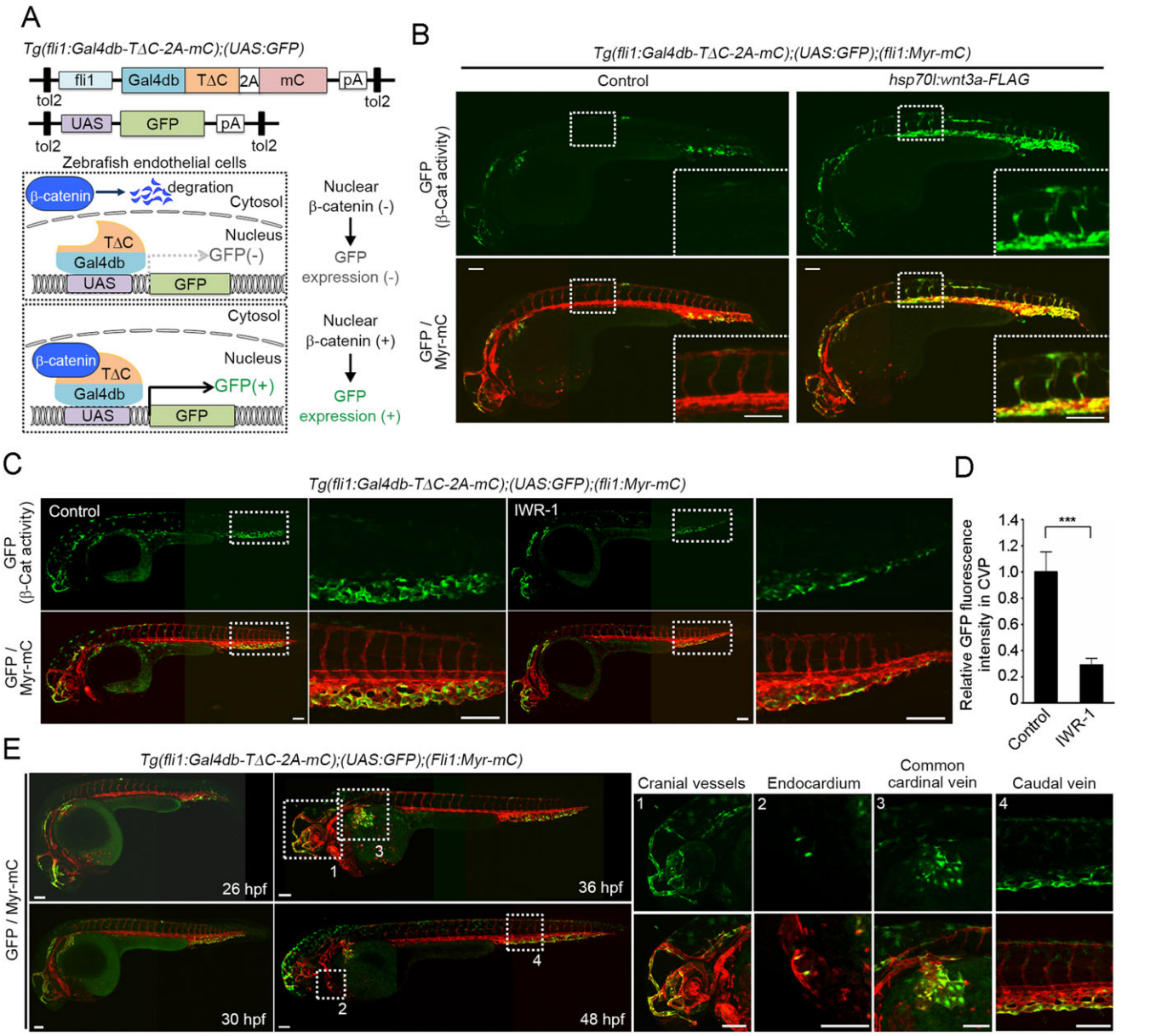

Fig. 1. Generation of an endothelial cell-specific β-catenin reporter zebrafish line. (A) Schematic representation of the endothelial cell (EC)-specific β-catenin reporter system. (Top) The constructs used to generate the EC-specific β-catenin reporter zebrafish line; (bottom) how the system works. In the absence of upstream signaling, β-catenin undergoes proteasomal degradation in the cytoplasm. Upon induction of the signaling that promotes β-catenin stabilization, β-catenin translocates to the nucleus and binds Gal4db-TΔC, thereby inducing GFP expression. Thus, this fluorescence reflects the transcriptional activity of β-catenin in ECs. Gal4db, DNA-binding domain of Gal4; TΔC, β-catenin-binding domain of Tcf4; 2A, 2A peptide sequence; mC, mCherry; pA, polyadenylation signal; UAS, upstream activation sequence. (B) 3D-rendered confocal stack fluorescence images of 32 hpf *Tg(fli1:Gal4db-TΔC-2A-mC);(UAS:GFP);(fli1:Myr-mC)* embryos injected without (control) or with *hsp70l:wnt3a-FLAG* plasmid and heat shocked at 22 hpf for 1 h. (Top) GFP images (β-catenin activity); (bottom) merged images (GFP/Myr-mC) of GFP (green) and mCherry (red). The boxed areas are enlarged in the insets. All confocal fluorescence images are lateral views with anterior to the left unless otherwise described. Myr-mC, myristoylation signal-tagged mCherry. (C) Confocal images of embryos treated with vehicle (control) or IWR-1, an axin-stabilizing compound, from 15-36 hpf, as in B. The boxed areas are enlarged to the right. (D) Fluorescence intensity of GFP in the caudal vein plexus (CVP), as observed in C, relative to that observed in vehicle-treated embryos. Data are mean±s.e.m. Control, n=7; IWR-1, n=11. ***P<0.001. (E) Merged fluorescence images (GFP/Myr-mC) of GFP (green) and mCherry (red) in *Tg(fli1:Gal4db-TΔC-2A-mC);(UAS:GFP);(fli1:Myr-mC)* embryos at 26, 30, 36 and 48 hpf. The boxed areas labeled 1-4 are enlarged to the right, showing (top) GFP images (β-catenin activity) and (bottom) merge of GFP (green) and mCherry (red) (GFP/Myr-mC). Note that green signal that does not overlap with mCherry fluorescence is background autofluorescence of the zebrafish embryos. Panels B, C and E are composites of two or three images, since it was not possible to capture the whole animal at sufficiently high resolution in a single field of view. Scale bars: 100 µm.

starting with Wnt as the canonical stimulator of β-catenin activity. To inhibit Wnt signaling, we ubiquitously expressed the Wnt antagonist Dickkopf 1 (Dkk1) in the *Tg(hsp70l:dkk1-FLAG)* and *Tg(hsp70l:dkk1-GFP)* lines by activating the *hsp70l* heat shock promoter. When heat shocked at 12 hpf, these Tg embryos displayed a short body axis phenotype (supplementary material Fig. S3A-E), as previously reported (Caneparo et al., 2007). Embryos heat shocked at 24 hpf exhibited caudal fin defects, indicating that Wnt signaling can be functionally inhibited by heat shock promoter-driven expression of Dkk1. However, Dkk1

Development (2015) 142, 497-509 doi:10.1242/dev.115576

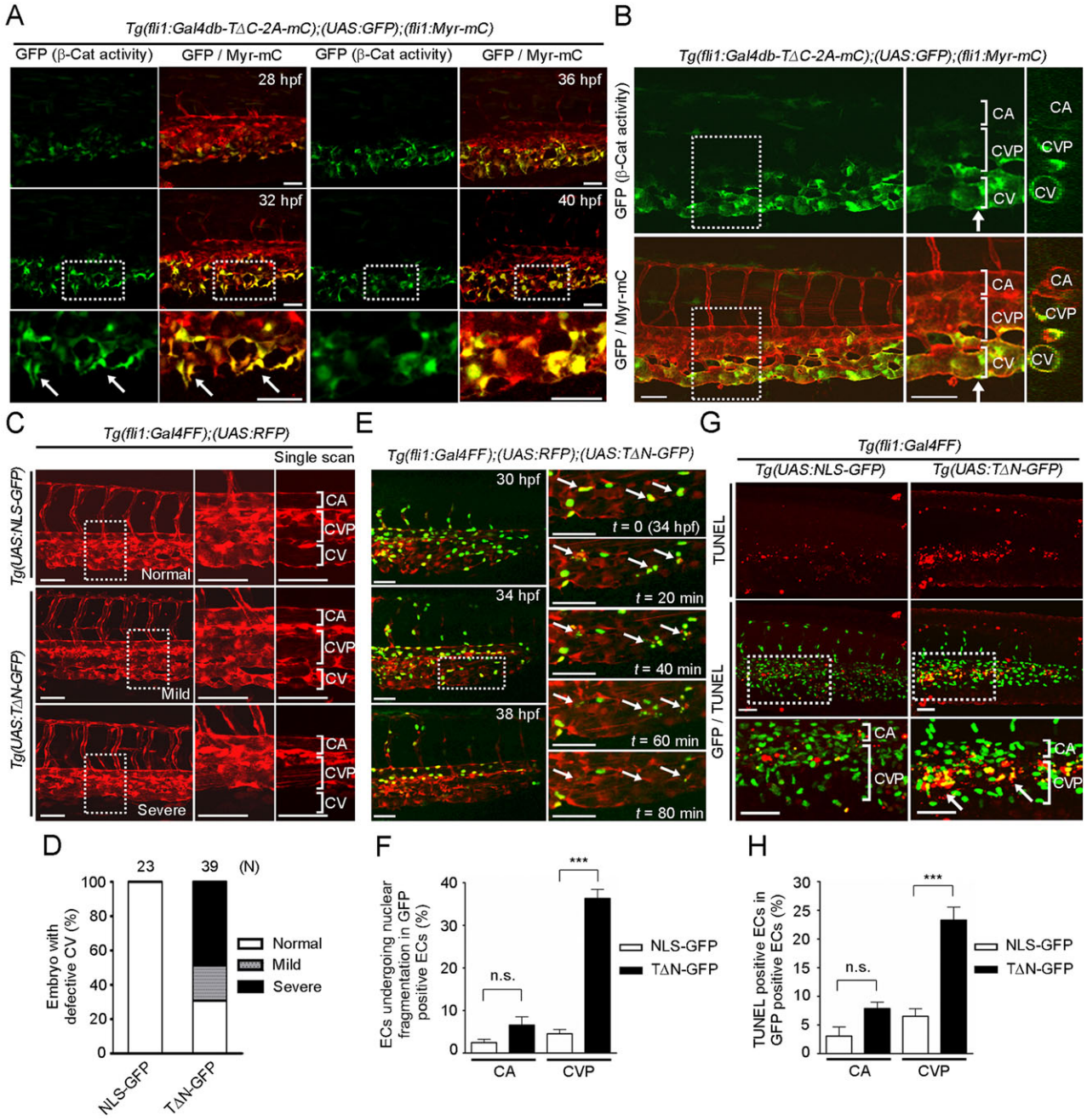

Fig. 2. β-catenin-dependent gene expression is required for CV formation. (A) Confocal fluorescence images of a *Tg(fli1:Gal4db-TΔC-2A-mC);(UAS:GFP);(fli1:Myr-mC)* embryo at 28 hpf and subsequent time-lapse images at the indicated time points. (Left) GFP images (β-catenin activity); (right) merge (GFP/Myr-mC) of GFP (green) and mCherry (red). The boxed areas are enlarged beneath. Arrows indicate β-catenin-dependent transcriptionally active ECs that sprout from the CV primordia. (B) Confocal images of the embryo at 48 hpf, as in Fig. 1B. The boxed areas are enlarged in the center; transverse sections at the arrows are shown to the right. (C) Confocal stack RFP fluorescence images of 48 hpf *Tg(UAS:NLS-GFP)* and *Tg(UAS:TΔN-GFP)* embryos with the *Tg(fli1:Gal4FF);(UAS:RFP)* background. The boxed areas are enlarged (center) and single scanned (right). Note that expression of dominant-negative Tcf, TΔN-GFP, in ECs caused a variety of impairments in CV formation. Embryos with the mild phenotype exhibited no blood circulation in the CV (middle row), whereas those with the severe phenotype lacked the CV (bottom row). Gal4FF, Gal4 DNA-binding domain fused to a duplicated portion of the VP16 transcriptional activation domain; NLS-GFP, nuclear localization signal-tagged GFP. (D) Quantification of the CV phenotypes observed in C, showing the percentage of normal embryos and those with mild and severe phenotypes. The number of embryos analyzed is indicated at the top. (E) Time-lapse confocal imaging of a *Tg(fli1:Gal4FF);(UAS:RFP);(UAS:TΔN-GFP)* embryo from 30-38 hpf. The merged GFP (green) and RFP (red) images at 30, 34 and 38 hpf are shown in the left column. In the right column, the boxed area in the 34 hpf image is enlarged and subsequent time-lapse images are shown. Arrows indicate ECs undergoing nuclear fragmentation. (F) Percentage of NLS-GFP-expressing and TΔN-GFP-expressing ECs that undergo nuclear fragmentation in the CA and CVP between 30 and 38 hpf. Data are expressed as a percentage of the total number of NLS-GFP-expressing and TΔN-GFP-expressing ECs, and shown as mean±s.e.m. NLS-GFP, n=5; TΔN-GFP, n=6. (G) Confocal stack fluorescence images of the 32 hpf *Tg(fli1:Gal4FF);(UAS:NLS-GFP)* (left) and *Tg(fli1:Gal4FF);(UAS:TΔN-GFP)* (right) embryos with TUNEL staining. Arrows indicate TUNEL-positive ECs that express TΔN-GFP. (H) Percentage of TUNEL-positive cells among the NLS-GFP- or TΔN-GFP-expressing ECs in the CA and CVP at 32 hpf. Data are mean±s.e.m. NLS-GFP, n=10; TΔN-GFP, n=9. CA, caudal artery; CV, caudal vein; CVP, caudal vein plexus. (F,H) ***P<0.01; n.s., not significant. Scale bars: 50 µm.

Development (2015) 142, 497-509 doi:10.1242/dev.115576

expression affected neither CV formation nor β-catenin transcriptional activity in the CV (Fig. 3A,B), suggesting that Wnt is not involved in β-catenin activation during CV formation.

We next focused on Bmp signaling, as Bmp regulates sprouting angiogenesis in CV development (Wiley et al., 2011). To investigate the role of Bmp in β-catenin-mediated CV formation, EC-specific β-catenin reporter fish embryos were injected with *hsp70l:noggin3* plasmid at the one-cell stage and heat shocked at 24 hpf. Overexpression of the Bmp antagonist Noggin 3 suppressed the transcriptional activity of β-catenin in the CV primordia and the ECs that had just sprouted from the CV primordia at 28 hpf (supplementary material Fig. S3F,G). At 36 hpf, Noggin 3-overexpressing embryos exhibited impaired CVP formation and decreased transcriptional activity of β-catenin in the defective CVP (Fig. 3C,D). By contrast, heat shock promoter-mediated overexpression of Bmp2b resulted in ectopic sprouting of venous ECs from the CVP (Fig. 3C). Importantly, β-catenin-dependent transcriptional activity was clearly observed in these ectopic vessels (Fig. 3C). Furthermore, the number of apoptotic ECs in the CVP was significantly increased by Noggin 3 (Fig. 3E,F). These findings reveal that Bmp stimulates β-catenin activity to regulate CV formation by promoting the survival of venous ECs.

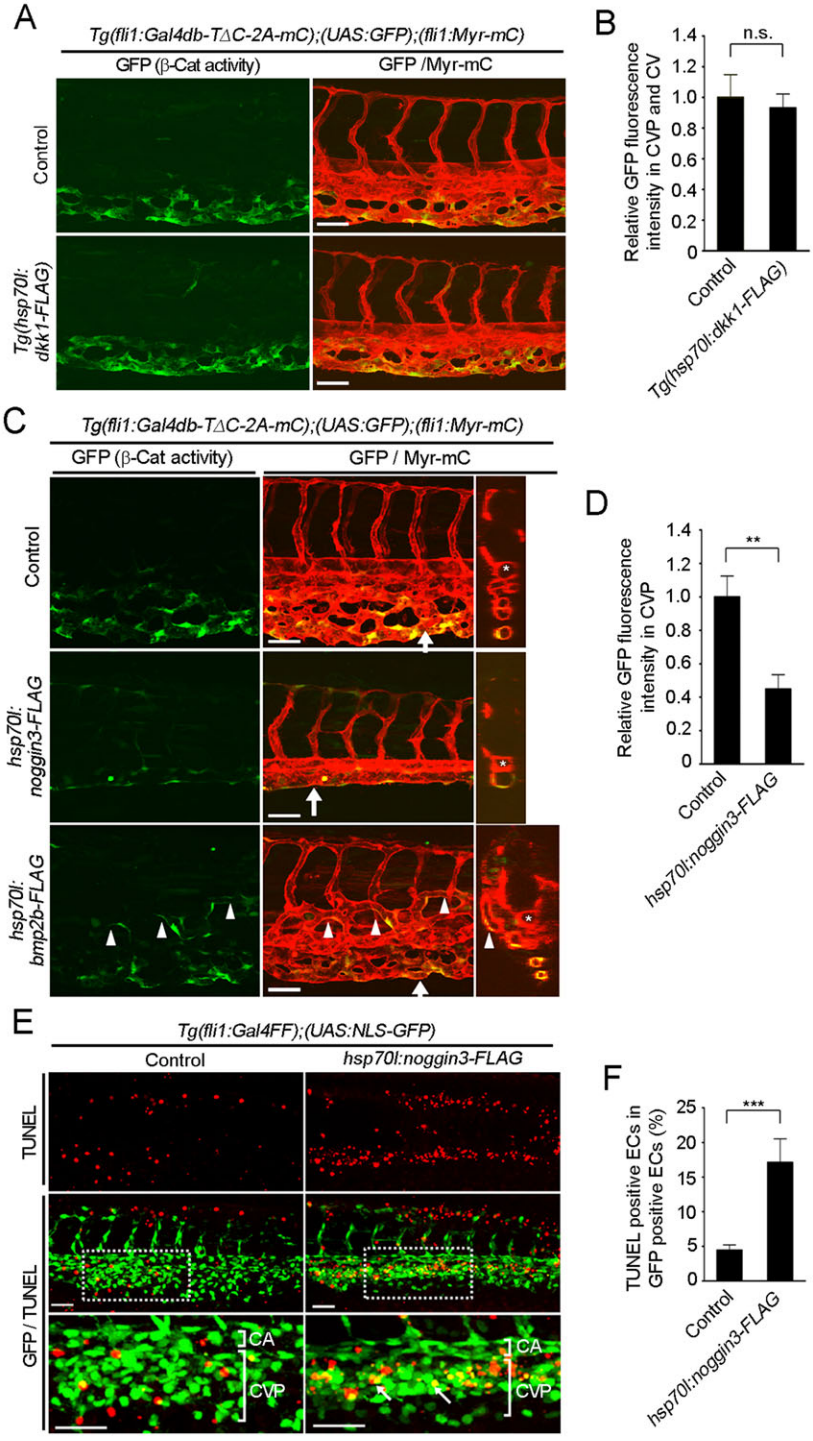

Fig. 3. Bmp stimulates β-catenin transcriptional activity in ECs to regulate CV formation. (A) Confocal fluorescence images of 48 hpf control (no additional *Tg*) and *Tg(hsp70l:dkk1-FLAG)* embryos with the *Tg(fli1:Gal4db-TΔC-2A-mC);(UAS:GFP);(fli1:Myr-mC)* background heat shocked at 24 hpf for 1 h. (B) Fluorescence intensity of GFP in the CV and CVP, as observed in A, relative to that in control embryos. Data are mean±s.e.m. Control, *n*=7; *Tg(hsp70l:dkk1-FLAG)*, *n*=9. (C) Confocal stack fluorescence images of 36 hpf embryos injected without (control) or with *hsp70l:noggin3-FLAG* or *hsp70l:bmp2b-FLAG* plasmid and heat shocked at 24 hpf for 1 h, as in A. Transverse sections at the arrows are shown to the right. Arrowheads indicate ectopic venous vessels originating from the CVP. Asterisks indicate CA. (D) Fluorescence intensities of GFP in the CVP of control and *hsp70l:noggin3-FLAG*-injected embryos, as observed in C, relative to that in control embryos. Data are mean±s.e.m. Control, *n*=6; *hsp70l:noggin3-FLAG*, *n*=8. (E) Confocal images of 32 hpf *Tg(fli1:Gal4FF);(UAS:NLS-GFP)* embryos injected without (control) or with *hsp70l:noggin3-FLAG* plasmid, heat shocked at 24 hpf and subjected to TUNEL staining, as in Fig. 2G. (F) Percentage of TUNEL-positive cells among NLS-GFP-expressing ECs in the CVP of the control and *hsp70l:noggin3-FLAG*-injected embryos as observed in E. Data are mean±s.e.m. Control, *n*=15; *hsp70l:noggin3-FLAG*, *n*=15. (B,D,F) $^{**}P<0.01$, $^{***}P<0.001$; n.s., not significant. Scale bars: 50 µm.

Development (2015) 142, 497-509 doi:10.1242/dev.115576

Vascular endothelial growth factor A (Vegfa) stimulates sprouting angiogenesis from the CA (Wiley et al., 2011). Thus, we hypothesized that Vegfa might promote EC survival in the CA. Treatment with Ki 8457 (Kwon et al., 2013), a Vegfa receptor inhibitor, induced nuclear fragmentation of ECs in the CA and intersegmental vessels (ISVs), but not in the CVP (supplementary material Fig. S4). These results indicate that distinct signaling pathways regulate EC survival in the CVP and CA; Bmp promotes EC survival in the CVP through β-catenin, whereas Vegfa maintains EC survival in the CA.

Involvement of Aggf1 in Bmp-induced CV formation

To address how Bmp stimulates β-catenin transcriptional activity and to identify the β-catenin target genes responsible for CV formation, we performed RNA-seq analyses. To identify the genes that are upregulated and downregulated in the ECs with high β-catenin transcriptional activity, GFP-positive and mCherry-positive [β-catenin (+)] ECs and GFP-negative and mCherry-positive [β-catenin (−)] ECs were isolated from the caudal parts of *Tg(fli1:Gal4db-TΔC-2A-mC);(UAS:GFP);(fli1:Myr-mC)* embryos and subjected to RNA-seq analyses (supplementary material Fig. S5). As expected, the β-catenin (+) ECs expressed high levels of β-catenin/Tcf target genes, such as *axin2*, *ccnd2a*, *ccnd2b*, *ctnnb1* and *tcf7* (Bandapalli et al., 2009; Kioussi et al., 2002; Lustig et al., 2002; Roose et al., 1999) (Table 1). In addition, some of the Bmp signal-responsive genes, such as *id1*, *id2a*, *id2b*, *smad6a* and *smad6b*, were highly expressed in the β-catenin (+) ECs (Hollnagel et al., 1999; Ishida et al., 2000) (Table 1), suggesting that β-catenin activity is stimulated by Bmp during CV development. Moreover, venous markers, including *dab2*, *ephb4a*, *ephb4b*, *flt4*, *nrp2a* and *nr2f2*, were highly expressed in the β-catenin (+) ECs (Covassin et al., 2006; Herzog et al., 2001; Sprague et al., 2006; Swift and Weinstein, 2009) (Table 1), suggesting that β-catenin plays a role in venous vessel development.

Analyzing the RNA-seq data revealed that the level of *aggf1* expression is higher in β-catenin (+) ECs than in β-catenin (−) ECs (Table 1). *AGGF1* was first described as a gene encoding an angiogenic factor and has been implicated as a causative gene for

Table 1. RNA-seq analysis of β-catenin (+) and β-catenin (−) ECs

			Reads*		
ENSDARG ID	Gene	Description	β-catenin (+)	β-catenin (−)	β-catenin (+)/(−)
β-catenin target genes					
00000014147	*axin2*	axin 2 (conductin, axil)	35.90	13.61	2.64
00000035750	*ccnd1*	cyclin D1	7.26	39.96	0.18
00000051748	*ccnd2a*	cyclin D2, a	103.38	34.73	2.98
00000070408	*ccnd2b*	cyclin D2, b	5.58	0.48	11.74
00000014571	*ctnnb1*	catenin (cadherin-associated protein), beta 1	211.49	90.53	2.34
00000038672	*tcf7*	transcription factor 7 (T-cell specific, HMG-box)	15.62	0.41	37.74
Bmp target genes					
00000040764	*id1*	inhibitor of DNA binding 1	300.78	133.97	2.25
00000055283	*id2a*	inhibitor of DNA binding 2, dominant negative helix-loop-helix protein, a	50.27	35.72	1.41
00000029544	*id2b*	inhibitor of DNA binding 2, dominant negative helix-loop-helix protein, b	13.39	1.46	9.15
00000053209	*smad6a*	SMAD family member 6a	38.19	5.22	7.32
00000031763	*smad6b*	SMAD family member 6b	47.06	12.60	3.73
Venous markers					
00000031761	*dab2*	disabled homolog 2 (Drosophila)	665.81	151.85	4.38
00000040346	*ephb4a*	eph receptor B4a	33.73	17.40	1.94
00000027112	*ephb4b*	eph receptor B4b	21.06	10.44	2.02
00000015717	*flt4*	fms-related tyrosine kinase 4	219.98	65.56	3.36
00000031622	*nrp2a*	neuropilin 2a	88.58	7.02	12.63
00000040926	*nr2f2*	nuclear receptor subfamily 2, group F, member 2	115.28	8.94	12.89
Arterial markers					
00000020164	*efnb2a*	ephrin B2a	4.82	17.12	0.28
00000074050	*efnb2b*	ephrin B2b	1.91	24.94	0.08
00000017321	*kdr*	kinase insert domain receptor (a type III receptor tyrosine kinase)	8.30	8.27	1.00
00000015815	*kdrl*	kinase insert domain receptor like	102.00	107.25	0.95
EC markers					
00000075549	*cdh5*	cadherin 5	78.02	48.07	1.62
00000054632	*fli1a*	friend leukemia integration 1a	342.49	189.36	1.81
00000019371	*flt1*	fms-related tyrosine kinase 1	4.14	10.56	0.39
00000028663	*tie2* (*tek*)	endothelium-specific receptor tyrosine kinase 2	145.26	57.03	2.55
Others					
00000037746	*actb1*	actin, beta 1	4958.56	4414.23	1.12
00000060109	*aggf1*	angiogenic factor with G patch and FHA domains 1	29.11	7.65	3.80
00000011941	*bmpr2a*	bone morphogenetic protein receptor, type II a (serine/threonine kinase)	24.60	2.73	9.01
00000019728	*bmpr1aa*	bone morphogenetic protein receptor, type 1aa	2.20	2.30	0.96

*Reads per kilobase of exon per million mapped reads.

Development (2015) 142, 497-509 doi:10.1242/dev.115576

Klippel–Trenaunay syndrome (KTS), a disorder characterized by venous malformation and hypertrophy of bones and soft tissues (Tian et al., 2004). It was recently reported that Aggf1 mediates the specification of venous EC identity in zebrafish embryos (Chen et al., 2013). Importantly, Major et al. also characterized AGGF1 as a nuclear chromatin-associated protein that participates in β-catenin-mediated transcription in human colon cancer cells (Major et al., 2008). Therefore, we hypothesized that Aggf1 acts downstream of Bmp to stimulate β-catenin transcriptional activity during CV development. To address this possibility, we examined the expression pattern of *aggf1* mRNA in zebrafish embryos. At 24, 30 and 36 hpf, *aggf1* mRNA was predominantly expressed in the

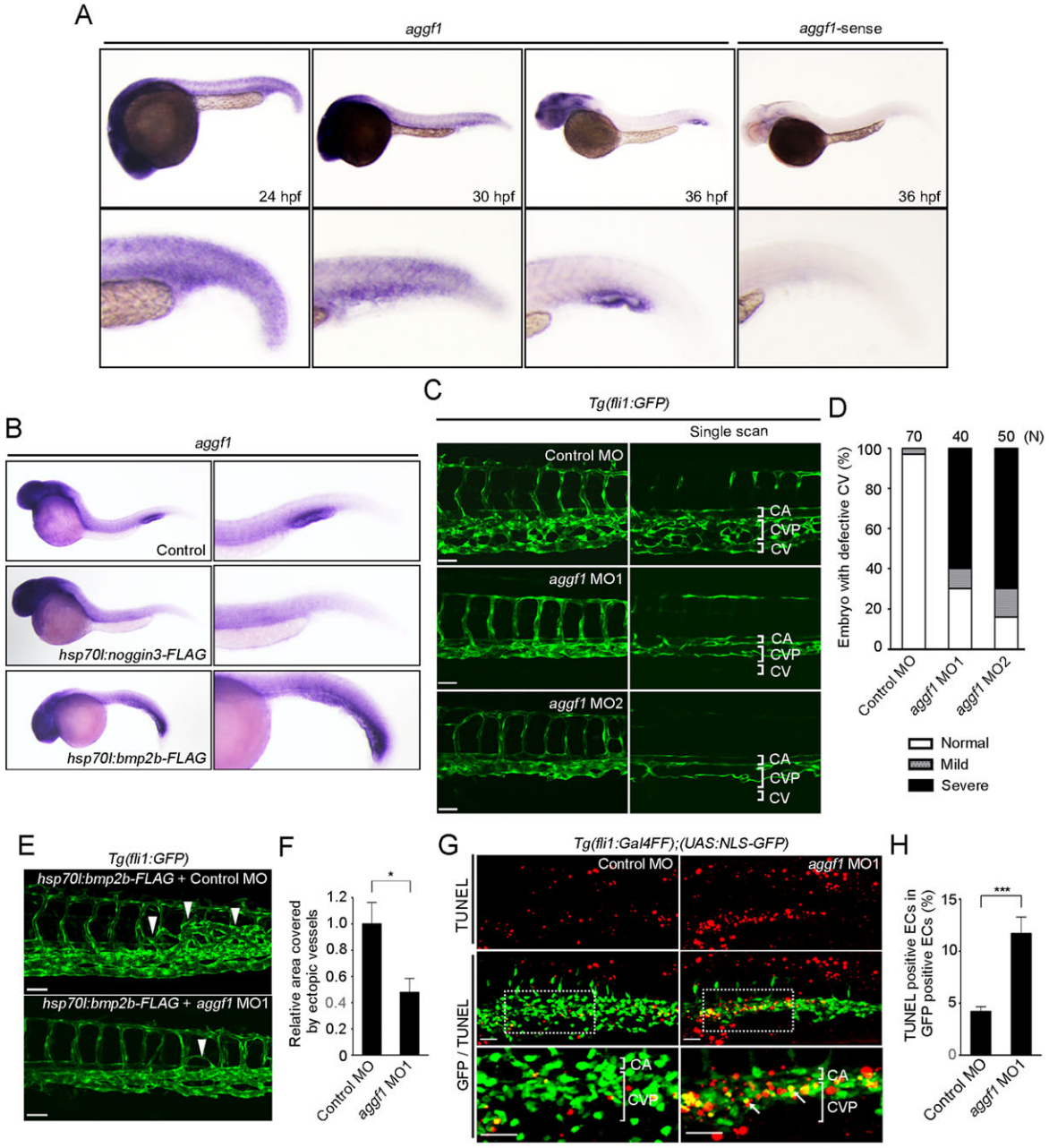

Fig. 4. Aggf1 is involved in Bmp-mediated CV formation. (A) Expression patterns of *aggf1* mRNA in zebrafish embryos at 24, 30 and 36 hpf, as detected by whole-mount *in situ* hybridization. Sense probe was used to confirm the specificity of the hybridization reaction. Regions from the yolk tube to the tail are enlarged beneath. (B) Expression of *aggf1* mRNA in 36 hpf embryos injected without (control) or with *hsp70l:noggin3-FLAG* or *hsp70l:bmp2b-FLAG* plasmid and heat shocked at 24 hpf. The caudal regions are enlarged to the right. (C) Confocal stack GFP images of the caudal region of 48 hpf *Tg(fli1:GFP)* embryos injected with control morpholino oligonucleotide (MO) or two independent MOs against *aggf1* (MO1 and MO2). Single-scan confocal images of these embryos are shown to the right. (D) The CV phenotypes observed in C were quantified as in Fig. 2D. (E) Confocal stack images of the caudal region of 48 hpf *Tg(fli1:GFP)* embryos injected with *hsp70l:bmp2b-FLAG* plasmid together with either control MO or *aggf1* MO1. Arrowheads indicate ectopic venous vessels originating from the CVP. (F) Quantification of ectopic venous vessel formation observed in E, showing the area covered by ectopic venous vessels relative to that in control MO-injected embryos. Data are mean±s.e.m. Control MO, *n*=10; *aggf1*, MO1 *n*=10. (G) Confocal stack fluorescence images of 32 hpf *Tg(fli1:Gal4FF);(UAS:NLS-GFP)* embryos injected with control MO or *aggf1* MO1 and subjected to TUNEL staining, as in Fig. 2G. (H) Percentage of TUNEL-positive ECs among the NLS-GFP-expressing ECs in the CVP of embryos injected with either control MO or *aggf1* MO1 as observed in G. Data are mean±s.e.m. Control MO, *n*=16; *aggf1* MO1, *n*=16. (F,H) **P*<0.05, ****P*<0.001; n.s., not significant. Scale bars: 50 µm.

Development (2015) 142, 497-509 doi:10.1242/dev.115576

head region (Fig. 4A), as previously reported (Chen et al., 2013). Additionally, its expression was weakly but broadly detected in the trunk region at 24 hpf, and had become more restricted to the vasculature by 30 hpf (Fig. 4A). At 36 hpf, *aggf1* expression was confined to the CVP, where β-catenin-mediated transcription actively occurred (Fig. 2A, Fig. 4A). Importantly, *aggf1* expression in the CVP was suppressed by Noggin 3, whereas its expression domain was expanded in Bmp2b-overexpressing embryos (Fig. 4B). These results indicate that Bmp induces *aggf1* expression in the CVP.

We next investigated whether Aggf1 is responsible for CV formation. Depletion of Aggf1 by two independent morpholino oligonucleotides (MOs) resulted in CV absence and defective CVP formation (Fig. 4C,D). Co-depletion of p53 (also known as Tp53) did not alleviate the CV defects caused by Aggf1 deficiency, although it partially rescued the defective formation of the CVP (supplementary material Fig. S6A,B), indicating that the phenotypes of *aggf1* morphants are not due to any MO off-target effects. By contrast, CA formation was unaffected by knockdown of Aggf1 (Fig. 4C; supplementary material Fig. S6A). Although the *aggf1* morphants showed some ISV defects, more than 80% of defective ISVs were venous vessels that sprouted from the CVP (venous ISVs, 83.3%; arterial ISVs, 16.7%; n=30) (supplementary material Fig. S6C), suggesting a role of Aggf1 in venous vessel development. Consistent with this, the ectopic formation of venous vessels induced by overexpression of Bmp2b was suppressed by the depletion of Aggf1 (Fig. 4E,F). Furthermore, *aggf1* morphants exhibited an increase in EC apoptosis in the CVP as compared with control MO-injected embryos (Fig. 4G,H). Collectively, these results indicate that Bmp induces Aggf1 expression to maintain the survival of venous ECs during CV formation.

The role of Aggf1 in Bmp-induced activation of β-catenin-dependent transcription

To investigate the role of Aggf1 in Bmp-induced activation of β-catenin transcriptional activity, we performed the luciferase assay using a Tcf-responsive reporter construct (TOPflash). Although Aggf1 alone did not stimulate the TOPflash reporter, it synergized with β-catenin to induce reporter gene expression (Fig. 5A). We also tested the effect of Aggf1 on the transcriptional activity of Gal4–β-catenin to explore whether Tcf is required for Aggf1-induced activation of β-catenin. Aggf1 potently increased the transcriptional activity of Gal4–β-catenin, but did not affect that of Gal4-VP16 (Fig. 5B). These

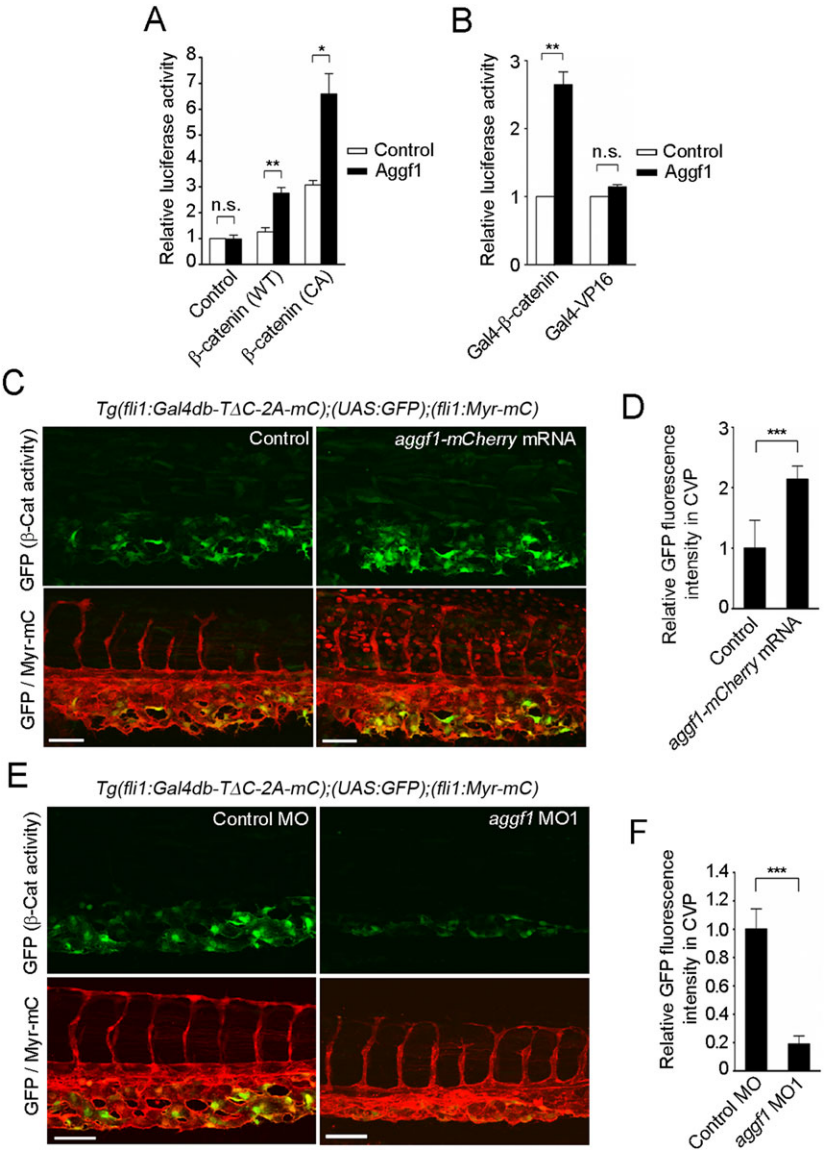

Fig. 5. Aggf1 functions downstream from Bmp to stimulate β-catenin transcriptional activity during CV formation. (A) Relative TOPflash/FOPflash activity in HEK 293 cells transfected with empty vector (control) or plasmid encoding either wild-type (WT) or constitutively active (CA) β-catenin together with the empty plasmid (control) or that expressing Aggf1. Data are shown relative to that in the empty vector-transfected cells, as the mean±s.e.m. of three independent experiments. (B) Relative luciferase activity in HEK 293 cells transfected with UAS-luciferase reporter and plasmid encoding either Gal4-β-catenin or Gal4-VP16 together with the empty plasmid (control) or that expressing Aggf1. Data are relative to that observed in the empty vector-transfected cells that express Gal4-β-catenin or Gal4-VP16, as the mean±s.e.m. of three independent experiments. (C) Confocal images of caudal regions of 36 hpf *Tg(fli1:Gal4db-TΔC-2A-mC);(UAS:GFP);(fli1:Myr-mC)* embryos injected without (control) or with *aggf1-mCherry* mRNA, as in Fig. 1B. (D) Fluorescence intensity of GFP in the CVP, as observed in C, relative to that observed in control embryos. Data are mean±s.e.m. Control, n=9; *aggf1-mCherry* mRNA, n=8. (E) Confocal images of caudal regions of 36 hpf *Tg(fli1:Gal4db-TΔC-2A-mC);(UAS:GFP);(fli1:Myr-mC)* embryos injected with control MO or *aggf1* MO1, as in Fig. 1B. (F) Fluorescence intensity of GFP in the CVP, as observed in E, relative to that observed in control MO-injected embryos. Data are mean±s.e.m. Control MO, n=11; *aggf1* MO1, n=12. (A,B,D,F) *P<0.05, **P<0.01, ***P<0.001; n.s., not significant. Scale bars: 50 µm.

Development (2015) 142, 497-509 doi:10.1242/dev.115576

findings suggest that Aggf1 stimulates the transcriptional activity of β-catenin by acting as a transcriptional co-factor.

We ascertained whether Aggf1 enhances β-catenin-mediated transcription *in vivo* by injecting *aggf1-mCherry* mRNA into EC-specific β-catenin reporter fish embryos. Overexpression of Aggf1-mCherry resulted in a significant increase in GFP in the CVP, although it did not induce ectopic GFP expression in other parts of the vasculature, indicating that Aggf1 enhances β-catenin transcription specifically in the CVP (Fig. 5C,D). We also found that depletion of Aggf1 suppressed β-catenin transcriptional activity in the defective CVP (Fig. 5E,F; supplementary material Fig. S6D,E). These findings suggest that Aggf1 acts downstream of Bmp to stimulate β-catenin transcriptional activity in the CVP.

Bmp-induced Nr2f2 expression through Aggf1-mediated activation of β-catenin

RNA-seq analyses revealed that *nr2f2* is highly induced in β-catenin (+) ECs (Table 1). Nr2f2 is an orphan nuclear receptor that plays a crucial role in venous specification (Aranguren et al., 2011; You et al., 2005). We investigated whether Bmp induces *nr2f2* expression to regulate CV formation. Expression of *nr2f2* was detected in both posterior cardinal veins (PCVs) and the CV in 48 hpf embryos (supplementary material Fig. S7A). Heat shock promoter-driven expression of Noggin 3 caused downregulation of *nr2f2* in the CV (Fig. 6A). By contrast, the expression domain of *nr2f2* in the CV was expanded by overexpression of Bmp2b (Fig. 6B), indicating that Bmp induces *nr2f2* expression in the CV.

We next explored the role of β-catenin in *nr2f2* expression. Expression of dominant-negative Tcf in ECs resulted in downregulation of *nr2f2* in the CV (Fig. 6C), suggesting that β-catenin plays a role in *nr2f2* expression. Consistent with this, the *NR2F2* expression level in human umbilical vein ECs was reduced by knockdown of β-catenin and increased by treatment with BIO (supplementary material Fig. S7B-D). We also investigated the involvement of Aggf1 in β-catenin-mediated *nr2f2* expression. The *nr2f2* expression level in the CV was decreased by depletion of Aggf1, but slightly increased by overexpression of Aggf1-mCherry (Fig. 6D,E). Importantly, treatment with BIO further augmented *nr2f2* expression in the CV of *aggf1-mCherry* mRNA-injected embryos (Fig. 6E). Collectively, these results indicate that Bmp induces *nr2f2* expression in the CV through Aggf1-mediated activation of β-catenin.

Crucial role of Nr2f2 in CV development

Next, we investigated the role of Nr2f2 in CV formation. Knockdown of Nr2f2 did not affect EC sprouting from the CV primordia and formation of the CVP (Fig. 6F,G). However, subsequent remodeling of the CVP was severely inhibited by depletion of Nr2f2, causing defective formation of the CV (Fig. 6H,I; supplementary material Fig. S8A-D). The CV defects caused by Nr2f2 deficiency were not rescued by co-depletion of p53, indicating that the phenotypes of *nr2f2* morphants are not due to MO off-target effects (supplementary material Fig. S8E,F). These results suggest that Nr2f2 is involved in CV formation. Unlike in the *aggf1* morphants, EC apoptosis in the CVP was not increased by Nr2f2 depletion, reflecting the non-essential role of Nr2f2 in β-catenin-promoted survival of venous ECs (supplementary material Fig. S9). However, knockdown of Nr2f2 caused downregulation of the venous marker *flt4* in the CVP without affecting expression of the endothelial marker *fli1a* (Fig. 6J,K). These results suggest that Nr2f2 promotes the differentiation of venous ECs required for CV development. Thus, β-catenin may regulate CV formation by promoting venous EC differentiation through Nr2f2 expression in addition to maintaining venous EC survival.

DISCUSSION

Analyses of EC-specific β-catenin knockout mice have confirmed the crucial role of β-catenin in vascular development. However, the precise function of β-catenin-mediated gene regulation in vascular development has not been clearly understood, since β-catenin regulates not only gene expression but also the formation of cell-cell junctions. Here, we have demonstrated a novel role of β-catenin in venous vessel development by generating a Tg zebrafish line that allows us to visualize EC-specific β-catenin transcriptional activity.

To date, several Tg animals have been developed to trace the transcriptional activity of β-catenin *in vivo* (DasGupta and Fuchs, 1999; Dorsky et al., 2002; Maretto et al., 2003; Moro et al., 2012; Shimizu et al., 2012). However, the reporter genes are ubiquitously expressed in these systems, making it difficult to study the function of β-catenin in a specific cell type or tissue. Our Tg line represents the first cell type-specific β-catenin reporter and as such is anticipated to contribute to a greater understanding of the diverse functions of β-catenin, since it is, at least in theory, applicable to any cell type or tissue.

GFP in the EC-specific β-catenin reporter line appears to reflect the transcriptional activity of β-catenin in ECs. It is noteworthy that this fluorescence is observed in venous ECs. However, this Tg line might not completely reproduce endogenous β-catenin activity in ECs. Although a previous report suggested that Wnt/β-catenin signaling promotes the proliferation of stalk cells during sprouting angiogenesis (Phng et al., 2009), we did not detect GFP signals in endothelial stalk cells. Therefore, the sensitivity of the EC-specific β-catenin reporter fish might not be high enough to detect weak transcriptional activity of β-catenin. However, at a minimum, the β-catenin-dependent transcription that we detected in this study reveals an essential role for β-catenin in CV formation.

Bmp signaling, but not Wnt, stimulates β-catenin transcriptional activity through Aggf1 to regulate CV development. Although Aggf1 was originally identified as a secreted angiogenic growth factor (Tian et al., 2004), it also functions in the nucleus to stimulate β-catenin-mediated gene expression (Major et al., 2008). Major et al. reported that AGGF1 associates with SWI/SNF chromatin remodeling complexes and participates in β-catenin-dependent transcription in human colon cancer cells (Major et al., 2008). Consistently, our study revealed that Aggf1 stimulates the transcriptional activity of β-catenin *in vitro* and *in vivo*. Thus, Aggf1 might act as a chromatin remodeling transcriptional co-factor for β-catenin. In addition to inducing the expression of Aggf1, Bmp might stabilize β-catenin and thereby lead to the induction of β-catenin-dependent transcription, since overexpression of Aggf1 enhanced β-catenin transcriptional activity and induced *nr2f2* expression only in the CVP, but not in the other vascular structures. Indeed, Bmp2 induces β-catenin accumulation in pulmonary artery ECs *in vitro* (de Jesus Perez et al., 2009). Further studies are needed to confirm these hypotheses.

Consistent with the role of Aggf1 in venous vessel formation, *AGGF1* is known to be mutated in KTS, a complex congenital disease characterized by varicosities and venous malformations of the lower limbs (Tian et al., 2004). Moreover, KTS patients develop hypertrophy of bones and soft tissues in addition to the venous abnormalities. It would be interesting to investigate whether AGGF1-mediated activation of β-catenin by Bmp is involved in the development of KTS.

Bmp promotes the survival of venous ECs through β-catenin-mediated gene expression during CV formation. A previous report

Development (2015) 142, 497-509 doi:10.1242/dev.115576

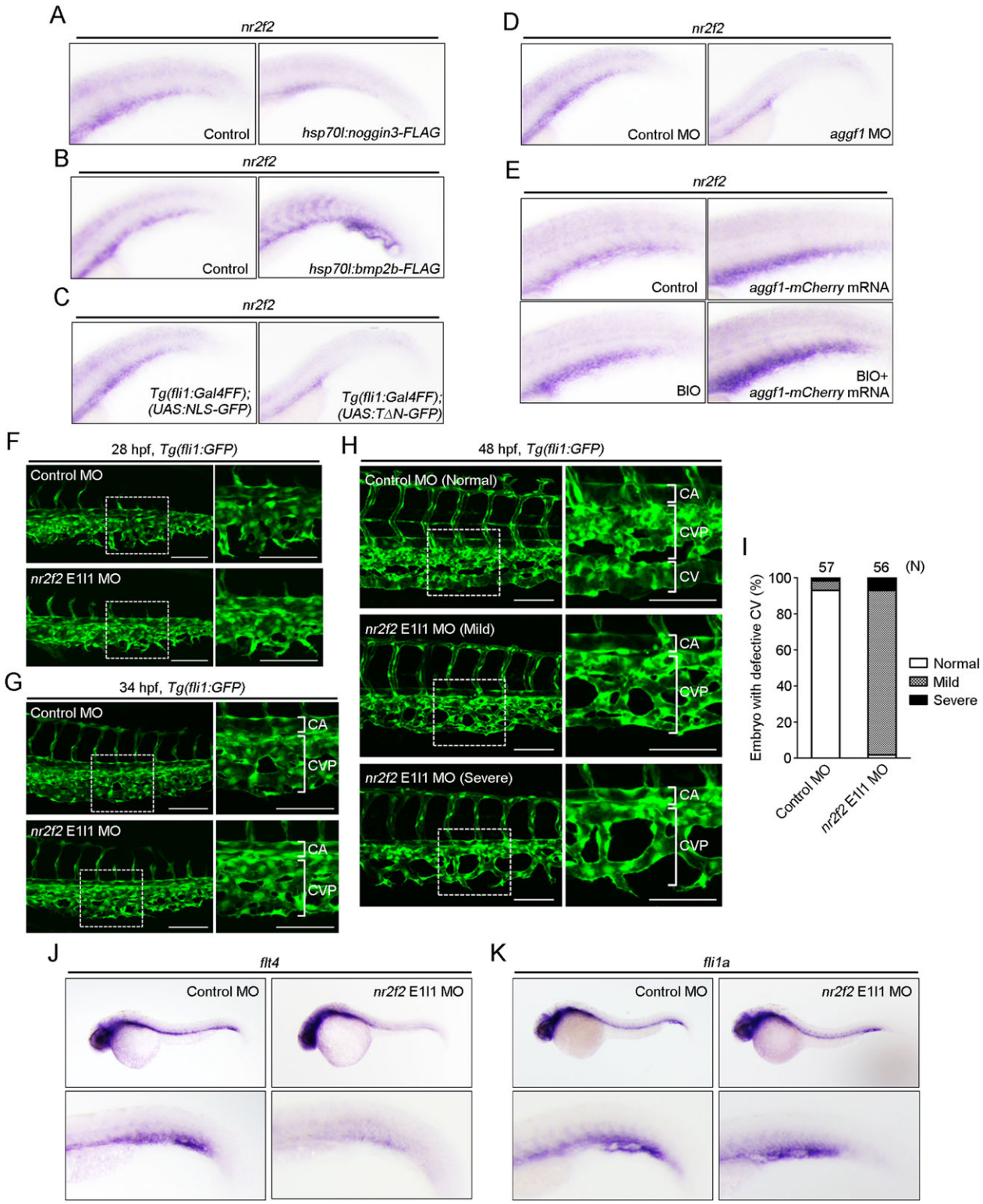

Fig. 6. Bmp regulates CV formation by inducing Nr2f2 expression via β-catenin. (A-E) Expression patterns of *nr2f2* mRNA in the caudal regions of 48 hpf embryos. (A) Embryos injected without (control) or with *hsp70l:noggin3-FLAG* plasmid were heat shocked at 24 hpf. (B) Embryos injected without (control) or with *hsp70l:bmp2b-FLAG* plasmid were heat shocked at 24 hpf. (C) *Tg(fli1:Gal4FF);(UAS:NLS-GFP)* and *Tg(fli1:Gal4FF);(UAS:TΔN-GFP)* embryos. (D) Embryos injected with control MO or *aggf1* MO. (E) Control embryos (top left) were injected with *aggf1-mCherry* mRNA, or incubated with BIO (a glycogen synthase kinase 3 inhibitor), or injected with *aggf1-mCherry* mRNA and then treated with BIO. (F-H) Confocal stack images of the caudal regions of *Tg(fli1:GFP)* embryos injected with control MO or *nr2f2* E1I1 MO at 28 (F), 34 (G) and 48 (H) hpf. The boxed areas are enlarged to the right. Note that knockdown of Nr2f2 caused a variety of impairments in CV formation. Embryos with the mild phenotype lacked the CV, but developed the CVP (middle row in H), whereas those with severe phenotypes lacked the CV and exhibited defective CVP (bottom row in H). (I) CV phenotypes observed in F were quantified, as in Fig. 2D. (J,K) Expression patterns of *flt4* (J) and *fli1a* (K) mRNAs in 36 hpf embryos injected with control MO or *nr2f2* E1I1 MO. Regions from the yolk tube to the tail are enlarged beneath. Scale bars: 100 µm.

Development (2015) 142, 497-509 doi:10.1242/dev.115576

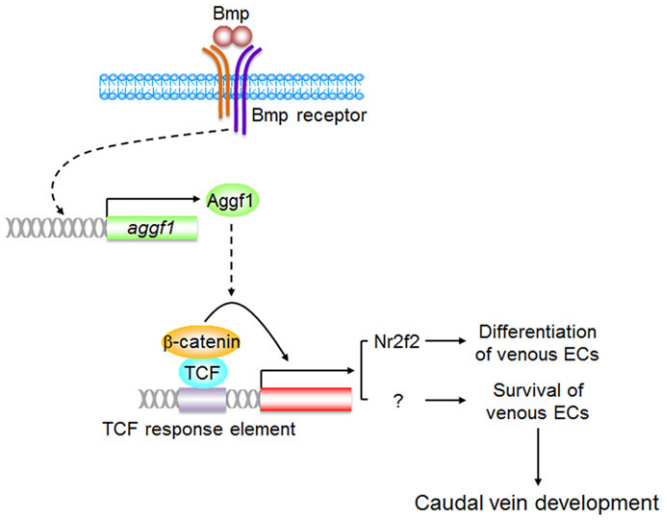

Fig. 7. Model for the mechanism underlying CV development. Bmp induces the expression of Aggf1 in ECs through an unknown mechanism. Subsequently, Aggf1 potentiates β-catenin transcriptional activity by acting as a transcriptional co-factor. Activated β-catenin regulates CV development by promoting the differentiation of venous ECs through expression of Nr2f2 and by maintaining the survival of venous ECs.

revealed that Bmp promotes the survival of pulmonary artery ECs through β-catenin-mediated expression of survivin (de Jesus Perez et al., 2009). However, our RNA-seq analyses did not detect the expression of *survivin* (*birc5a*) mRNA in β-catenin (+) ECs. Therefore, other target genes are likely be induced by β-catenin to promote the survival of venous ECs during CV formation.

β-catenin induces *nr2f2* expression in the CV. β-catenin has been shown to induce Nr2f2 expression in preadipocytes by acting directly on its −4.7 kb proximal promoter region (Okamura et al., 2009). However, our luciferase reporter gene analyses revealed that a 5 kb proximal zebrafish *nr2f2* promoter is not stimulated by active β-catenin. Therefore, β-catenin is likely to indirectly promote *nr2f2* expression in ECs during CV formation. In addition, β-catenin-dependent and -independent pathways might regulate *nr2f2* expression, as inhibition of β-catenin/Tcf-mediated transcription suppressed *nr2f2* expression in the CV but not in the PCV. Consistent with this, the chromatin remodeling enzyme BRG1 directly promotes murine *Nr2f2* expression independently of β-catenin (Davis et al., 2013). Furthermore, it was recently shown that *nr2f2* expression in the PCV depends on Sox7 and Sox18 (Swift et al., 2014). Therefore, different mechanisms of *nr2f2* expression might be employed in the CV and PCV.

β-catenin-mediated expression of Nr2f2 regulates the differentiation of venous ECs during CV development. Nr2f2 depletion resulted in downregulation of the venous marker *flt4* in the CVP, suggesting a role of Nr2f2 in venous EC specification. However, Nr2f2 is required for expression of some but not all markers of venous identity. For instance, expression of the venous markers *ephb4a* and *dab2* in the PCV is only partially affected by depletion of Nr2f2 in zebrafish (Aranguren et al., 2011; Swift et al., 2014). Similarly, levels of endothelial *Ephb4* are only slightly reduced in the cardinal vein of Nr2f2-deficient mice (You et al., 2005). Therefore, other factors, in addition to Nr2f2, might be required for full establishment of venous identity.

Although the present study showed that Bmp promotes venous EC differentiation through expression of Nr2f2, Bmp is also known to negatively regulate lymphatic development. Recently, Dunworth et al. reported that Bmp suppresses the expression of Prox1, a key regulator of lymphatic development, thereby preventing differentiation of lymphatic ECs (Dunworth et al., 2014). As such, Bmp might regulate venous vessel formation by inducing the differentiation of venous ECs through expression of Nr2f2 and by suppressing the differentiation of lymphatic ECs through downregulation of Prox1. However, the requirement of Nr2r2 for *prox1* expression in embryonic veins has also been reported (Srinivasan et al., 2010; Swift et al., 2014). Thus, further studies are needed to delineate the mechanisms by which Bmp regulates venous and lymphatic development.

In summary, we have successfully visualized the EC-specific transcriptional activity of β-catenin in living animals, and have uncovered a novel role for β-catenin in vascular development (Fig. 7). During CV formation, Bmp induces the expression of Aggf1 in ECs, which leads to the activation of β-catenin-mediated transcription. Activated β-catenin regulates CV formation by promoting the Nr2f2-dependent differentiation of venous ECs and by maintaining their survival.

MATERIALS AND METHODS

Zebrafish husbandry

Zebrafish (*Danio rerio*) were maintained and bred under standard conditions. Embryos were staged by hpf at 28°C (Kimmel et al., 1995). Animal experiments were approved by the animal committee of the National Cerebral and Cardiovascular Center and performed according to the regulations of the National Cerebral and Cardiovascular Center. Heat shock, MO and mRNA injections and chemical treatments of embryos were undertaken as described in the supplementary Materials and Methods.

Plasmid constructs

Expression constructs were generated as described in detail in the supplementary Materials and Methods.

Transgenic zebrafish lines

Tg(fli1:Gal4db-TΔC-2A-mC), *Tg(fli1:Myr-mC)*, *Tg(UAS:TΔN-GFP)*, *Tg(UAS:NLS-GFP)*, *Tg(flk1:NLS-Eos)*, *Tg(hsp70l:dkk1-FLAG)* and *Tg(flt1:mC)* zebrafish lines were generated according to the protocol described previously (Kwon et al., 2013). Other Tg lines were obtained as described in the supplementary Materials and Methods. Genotyping of the Tg lines was by genomic PCR as described in the supplementary Materials and Methods.

Image acquisition, processing and quantification

Zebrafish embryos were mounted in 1% low-melting agarose poured onto a 35-mm diameter glass-based dish (Asahi Techno Glass) as previously described (Fukuhara et al., 2014) (see supplementary Materials and Methods).

Confocal images were taken with a FluoView FV1000 confocal upright microscope system (Olympus) equipped with water-immersion 10× (LUMPlanFL, 0.30 NA) and 20× (XLUMPlanFL, 1.0 NA) lenses. The 473 nm and 559 nm laser lines were employed. For confocal time-lapse imaging, images were collected every 10-20 min for 5-12 h. To avoid cross-detection of green and red signals, images were acquired sequentially at 473 nm and 559 nm. *z*-stack images were 3D volume rendered with fluorescence mode employing Volocity 3D imaging analysis software (PerkinElmer).

Quantitative analyses of fluorescence intensity, CV defects and ectopic vessel formation were performed as described in the supplementary Materials and Methods.

FACS and RNA-seq analyses

Tg(fli1:Gal4db-TΔC-2A-mC);(UAS:GFP);(fli1:Myr-mC) fish embryos were cut along the dorsoventral axis as described in supplementary material Fig. S4. Caudal parts of the embryos were collected, incubated in 0.25% trypsin in phosphate-buffered saline at 28°C for 15 min, and dissociated by gentle pipetting. The dissociated cells were sorted using a FACS Aria III cell sorter (BD Biosciences) and grouped into GFP-positive

mCherry-positive [β-catenin (+)] and GFP-negative mCherry-positive [β-catenin (−)] EC populations.

Total RNA was purified from β-catenin (+) ECs and β-catenin (−) ECs using a NucleoSpin RNA XS kit (Macherey-Nagel) following the manufacturer's instructions, and subjected to RNA-seq analyses as described in the supplementary Materials and Methods. The RNA-seq data have been deposited at the Sequence Read Archive (SRA) database (NCBI) under accession number SRP051129.

Whole-mount *in situ* hybridization

Whole-mount *in situ* hybridization of zebrafish embryos was performed as described previously (Fukuhara et al., 2014).

TUNEL and luciferase reporter assays

EC apoptosis was quantified by TUNEL assay as described in the supplementary Materials and Methods. TOPflash reporter assays were carried out in HEK 293 cells as described in the supplementary Materials and Methods.

Statistical analysis

Data were analyzed using GraphPad Prism software. Data are expressed as the mean±s.e.m., as described in the figure legends. Statistical significance for paired samples and for multiple comparisons was determined by Student's *t*-test and by one-way analysis of variance with Tukey's test, respectively. Data were considered statistically significant at $P<0.05$.

Acknowledgements

We thank N. Lawson for the *fli1* promoter and *Tg(fli1:GFP)* fish; K. Kawakami for the Tol2 system and *Tg(UAS:GFP)* and *Tg(UAS:RFP)* fish lines; M. Affolter for *Tg(fli1:Gal4FF)* fish; M. Hibi for the UAS-GFP reporter and the Gal4FF plasmid; D. Y. Stainier for the *flk1* promoter; J. Kuwada for the *hsp70l* promoter; G. Felsenfeld for the chicken β-globin insulator; A. Kikuchi for the hTCF4 plasmid; K. Hiratomi, M. Sone, W. Koeda, E. Okamoto and T. Babazono for excellent technical assistance; and K. Shioya for excellent fish care.

Competing interests

The authors declare no competing or financial interests.

Author contributions

T.K., S.F., K.T. and N.M. conceived and designed the research; T.K., S.F., K.T., T.T., Y.W., K.A., H.N., H.F. and S.Y. carried out experiments and analyzed the data; Y.S. and A.G. supported the experiments performed by T.K.; T.K., S.F. and N.M. wrote the manuscript.

Funding

This work was supported in part by Grants-in-Aid for Scientific Research on Innovative Areas 'Fluorescence Live Imaging' [No. 22113009 to S.F.] and 'Neuro-Vascular Wiring' [No. 22122003 to N.M.] from The Ministry of Education, Culture, Sports, Science, and Technology, Japan; by Grants-in-Aid for Young Scientists (B) [No. 24790304 to K.T.], for Scientific Research (B) [No. 22390040 and No. 25293050 to S.F. and No. 24370084 to N.M.] and for Exploratory Research [No. 26670107 to S.F.] from the Japan Society for the Promotion of Science; by grants from the Ministry of Health, Labour, and Welfare of Japan (to N.M.) and by the Program to Disseminate Tenure Tracking System, MEXT, Japan (to K.T.); the Core Research for Evolutional Science and Technology (CREST) program of the Japan Science and Technology Agency (JST) (to N.M.); Takeda Science Foundation (to S.F., N.M.); the Naito Foundation (to S.F.); Mochida Memorial Foundation for Medical and Pharmaceutical Research (to S.F.); Japan Cardiovascular Research Foundation (to S.F.); and the Uehara Memorial Foundation (to K.T.).

Supplementary material

Supplementary material available online at
http://dev.biologists.org/lookup/suppl/doi:10.1242/dev.115576/-/DC1

References

Ahrens, M. J., Romereim, S. and Dudley, A. T. (2011). A re-evaluation of two key reagents for in vivo studies of Wnt signaling. *Dev. Dyn.* **240**, 2060-2068.

Al Alam, D., Green, M., Tabatabai Irani, R., Parsa, S., Danopoulos, S., Sala, F. G., Branch, J., El Agha, E., Tiozzo, C., Voswinckel, R. et al. (2011). Contrasting expression of canonical Wnt signaling reporters TOPGAL, BATGAL and Axin2 (LacZ) during murine lung development and repair. *PLoS ONE* **6**, e23139.

Angers, S. and Moon, R. T. (2009). Proximal events in Wnt signal transduction. *Nat. Rev. Mol. Cell Biol.* **10**, 468-477.

Aranguren, X. L., Beerens, M., Vandevelde, W., Dewerchin, M., Carmeliet, P. and Luttun, A. (2011). Transcription factor COUP-TFII is indispensable for venous and lymphatic development in zebrafish and Xenopus laevis. *Biochem. Biophys. Res. Commun.* **410**, 121-126.

Bandapalli, O. R., Dihlmann, S., Helwa, R., Macher-Goeppinger, S., Weitz, J., Schirmacher, P. and Brand, K. (2009). Transcriptional activation of the β-catenin gene at the invasion front of colorectal liver metastases. *J. Pathol.* **218**, 370-379.

Caneparo, L., Huang, Y.-L., Staudt, N., Tada, M., Ahrendt, R., Kazanskaya, O., Niehrs, C. and Houart, C. (2007). Dickkopf-1 regulates gastrulation movements by coordinated modulation of Wnt/β-catenin and Wnt/PCP activities, through interaction with the Dally-like homolog Knypek. *Genes Dev.* **21**, 465-480.

Cattelino, A., Liebner, S., Gallini, R., Zanetti, A., Balconi, G., Corsi, A., Bianco, P., Wolburg, H., Moore, R., Oreda, B. et al. (2003). The conditional inactivation of the β-catenin gene in endothelial cells causes a defective vascular pattern and increased vascular fragility. *J. Cell Biol.* **162**, 1111-1122.

Chen, B., Dodge, M. E., Tang, W., Lu, J., Ma, Z., Fan, C.-W., Wei, S., Hao, W., Kilgore, J., Williams, N. S. et al. (2009). Small molecule-mediated disruption of Wnt-dependent signaling in tissue regeneration and cancer. *Nat. Chem. Biol.* **5**, 100-107.

Chen, D., Li, L., Tu, X., Yin, Z. and Wang, Q. (2013). Functional characterization of Klippel-Trenaunay syndrome gene AGGF1 identifies a novel angiogenic signaling pathway for specification of vein differentiation and angiogenesis during embryogenesis. *Hum. Mol. Genet.* **22**, 963-976.

Choi, J., Mouillesseaux, K., Wang, Z., Fiji, H. D. G., Kinderman, S. S., Otto, G. W., Geisler, R., Kwon, O. and Chen, J.-N. (2011). Aplexone targets the HMG-CoA reductase pathway and differentially regulates arteriovenous angiogenesis. *Development* **138**, 1173-1181.

Clevers, H. (2006). Wnt/β-catenin signaling in development and disease. *Cell* **127**, 469-480.

Corada, M., Nyqvist, D., Orsenigo, F., Caprini, A., Giampietro, C., Taketo, M. M., Iruela-Arispe, M. L., Adams, R. H. and Dejana, E. (2010). The Wnt/β-catenin pathway modulates vascular remodeling and specification by upregulating Dll4/Notch signaling. *Dev. Cell* **18**, 938-949.

Covassin, L., Amigo, J. D., Suzuki, K., Teplyuk, V., Straubhaar, J. and Lawson, N. D. (2006). Global analysis of hematopoietic and vascular endothelial gene expression by tissue specific microarray profiling in zebrafish. *Dev. Biol.* **299**, 551-562.

Daneman, R., Agalliu, D., Zhou, L., Kuhnert, F., Kuo, C. J. and Barres, B. A. (2009). Wnt/β-catenin signaling is required for CNS, but not non-CNS, angiogenesis. *Proc. Natl. Acad. Sci. USA* **106**, 641-646.

DasGupta, R. and Fuchs, E. (1999). Multiple roles for activated LEF/TCF transcription complexes during hair follicle development and differentiation. *Development* **126**, 4557-4568.

Davis, R. B., Curtis, C. D. and Griffin, C. T. (2013). BRG1 promotes COUP-TFII expression and venous specification during embryonic vascular development. *Development* **140**, 1272-1281.

de Jesus Perez, V. A., Alastalo, T.-P., Wu, J. C., Axelrod, J. D., Cooke, J. P., Amieva, M. and Rabinovitch, M. (2009). Bone morphogenetic protein 2 induces pulmonary angiogenesis via Wnt-β-catenin and Wnt-RhoA-Rac1 pathways. *J. Cell Biol.* **184**, 83-99.

Dejana, E., Orsenigo, F. and Lampugnani, M. G. (2008). The role of adherens junctions and VE-cadherin in the control of vascular permeability. *J. Cell Sci.* **121**, 2115-2122.

Dorsky, R. I., Sheldahl, L. C. and Moon, R. T. (2002). A transgenic Lef1/β-catenin-dependent reporter is expressed in spatially restricted domains throughout zebrafish development. *Dev. Biol.* **241**, 229-237.

Dunworth, W. P., Cardona-Costa, J., Bozkulak, E. C., Kim, J.-D., Meadows, S., Fischer, J. C., Wang, Y., Cleaver, O., Qyang, Y., Ober, E. A. et al. (2014). Bone morphogenetic protein 2 signaling negatively modulates lymphatic development in vertebrate embryos. *Circ. Res.* **114**, 56-66.

Fukuhara, S., Zhang, J., Yuge, S., Ando, K., Wakayama, Y., Sakaue-Sawano, A., Miyawaki, A. and Mochizuki, N. (2014). Visualizing the cell-cycle progression of endothelial cells in zebrafish. *Dev. Biol.* **393**, 10-23.

Herzog, Y., Kalcheim, C., Kahane, N., Reshef, R. and Neufeld, G. (2001). Differential expression of neuropilin-1 and neuropilin-2 in arteries and veins. *Mech. Dev.* **109**, 115-119.

Hollnagel, A., Oehlmann, V., Heymer, J., Rüther, U. and Nordheim, A. (1999). Id genes are direct targets of bone morphogenetic protein induction in embryonic stem cells. *J. Biol. Chem.* **274**, 19838-19845.

Hurlstone, A. F. L., Haramis, A.-P. G., Wienholds, E., Begthel, H., Korving, J., van Eeden, F., Cuppen, E., Zivkovic, D., Plasterk, R. H. A. and Clevers, H. (2003). The Wnt/β-catenin pathway regulates cardiac valve formation. *Nature* **425**, 633-637.

Ishida, W., Hamamoto, T., Kusanagi, K., Yagi, K., Kawabata, M., Takehara, K., Sampath, T. K., Kato, M. and Miyazono, K. (2000). Smad6 is a Smad1/5-induced smad inhibitor. Characterization of bone morphogenetic protein-responsive element in the mouse Smad6 promoter. *J. Biol. Chem.* **275**, 6075-6079.

Kim, J.-D., Kang, H., Larrivée, B., Lee, M. Y., Mettlen, M., Schmid, S. L., Roman, B. L., Qyang, Y., Eichmann, A. and Jin, S.-W. (2012). Context-dependent proangiogenic function of bone morphogenetic protein signaling is mediated by disabled homolog 2. *Dev. Cell* **23**, 441-448.

Kimmel, C. B., Ballard, W. W., Kimmel, S. R., Ullmann, B. and Schilling, T. F. (1995). Stages of embryonic development of the zebrafish. *Dev. Dyn.* **203**, 253-310.

Kioussi, C., Briata, P., Baek, S. H., Rose, D. W., Hamblet, N. S., Herman, T., Ohgi, K. A., Lin, C., Gleiberman, A., Wang, J. et al. (2002). Identification of a Wnt/Dvl/β-Catenin→Pitx2 pathway mediating cell-type-specific proliferation during development. *Cell* **111**, 673-685.

Kwon, H.-B., Fukuhara, S., Asakawa, K., Ando, K., Kashiwada, T., Kawakami, K., Hibi, M., Kwon, Y.-G., Kim, K.-W., Alitalo, K. et al. (2013). The parallel growth of motoneuron axons with the dorsal aorta depends on Vegfc/Vegfr3 signaling in zebrafish. *Development* **140**, 4081-4090.

Liebner, S., Cattelino, A., Gallini, R., Rudini, N., Iurlaro, M., Piccolo, S. and Dejana, E. (2004). β-catenin is required for endothelial-mesenchymal transformation during heart cushion development in the mouse. *J. Cell Biol.* **166**, 359-367.

Liebner, S., Corada, M., Bangsow, T., Babbage, J., Taddei, A., Czupalla, C. J., Reis, M., Felici, A., Wolburg, H., Fruttiger, M. et al. (2008). Wnt/β-catenin signaling controls development of the blood-brain barrier. *J. Cell Biol.* **183**, 409-417.

Logan, C. Y. and Nusse, R. (2004). The Wnt signaling pathway in development and disease. *Annu. Rev. Cell Dev. Biol.* **20**, 781-810.

Lustig, B., Jerchow, B., Sachs, M., Weiler, S., Pietsch, T., Karsten, U., van de Wetering, M., Clevers, H., Schlag, P. M., Birchmeier, W. et al. (2002). Negative feedback loop of Wnt signaling through upregulation of conductin/axin2 in colorectal and liver tumors. *Mol. Cell. Biol.* **22**, 1184-1193.

MacDonald, B. T., Tamai, K. and He, X. (2009). Wnt/β-catenin signaling: components, mechanisms, and diseases. *Dev. Cell* **17**, 9-26.

Major, M. B., Roberts, B. S., Berndt, J. D., Marine, S., Anastas, J., Chung, N., Ferrer, M., Yi, X., Stoick-Cooper, C. L., von Haller, P. D. et al. (2008). New regulators of Wnt/β-catenin signaling revealed by integrative molecular screening. *Sci. Signal.* **1**, ra12.

Maretto, S., Cordenonsi, M., Dupont, S., Braghetta, P., Broccoli, V., Hassan, A. B., Volpin, D., Bressan, G. M. and Piccolo, S. (2003). Mapping Wnt/β-catenin signaling during mouse development and in colorectal tumors. *Proc. Natl. Acad. Sci. USA* **100**, 3299-3304.

Moro, E., Ozhan-Kizil, G., Mongera, A., Beis, D., Wierzbicki, C., Young, R. M., Bournele, D., Domenichini, A., Valdivia, L. E., Lum, L. et al. (2012). In vivo Wnt signaling tracing through a transgenic biosensor fish reveals novel activity domains. *Dev. Biol.* **366**, 327-340.

Okamura, M., Kudo, H., Wakabayashi, K.-i., Tanaka, T., Nonaka, A., Uchida, A., Tsutsumi, S., Sakakibara, I., Naito, M., Osborne, T. F. et al. (2009). COUP-TFII acts downstream of Wnt/β-catenin signal to silence PPARγ gene expression and repress adipogenesis. *Proc. Natl. Acad. Sci. USA* **106**, 5819-5824.

Phng, L.-K., Potente, M., Leslie, J. D., Babbage, J., Nyqvist, D., Lobov, I., Ondr, J. K., Rao, S., Lang, R. A., Thurston, G. et al. (2009). Nrarp coordinates endothelial Notch and Wnt signaling to control vessel density in angiogenesis. *Dev. Cell* **16**, 70-82.

Roose, J., Huls, G., van Beest, M., Moerer, P., van der Horn, K., Goldschmeding, R., Logtenberg, T. and Clevers, H. (1999). Synergy between tumor suppressor APC and the β-catenin-Tcf4 target Tcf1. *Science* **285**, 1923-1926.

Shimizu, N., Kawakami, K. and Ishitani, T. (2012). Visualization and exploration of Tcf/Lef function using a highly responsive Wnt/β-catenin signaling-reporter transgenic zebrafish. *Dev. Biol.* **370**, 71-85.

Sprague, J., Bayraktaroglu, L., Clements, D., Conlin, T., Fashena, D., Frazer, K., Haendel, M., Howe, D. G., Mani, P., Ramachandran, S. et al. (2006). The Zebrafish Information Network: the zebrafish model organism database. *Nucleic Acids Res.* **34** Suppl. 1, D581-D585.

Srinivasan, R. S., Geng, X., Yang, Y., Wang, Y., Mukatira, S., Studer, M., Porto, M. P. R., Lagutin, O. and Oliver, G. (2010). The nuclear hormone receptor Coup-TFII is required for the initiation and early maintenance of Prox1 expression in lymphatic endothelial cells. *Genes Dev.* **24**, 696-707.

Stenman, J. M., Rajagopal, J., Carroll, T. J., Ishibashi, M., McMahon, J. and McMahon, A. P. (2008). Canonical Wnt signaling regulates organ-specific assembly and differentiation of CNS vasculature. *Science* **322**, 1247-1250.

Swift, M. R. and Weinstein, B. M. (2009). Arterial-venous specification during development. *Circ. Res.* **104**, 576-588.

Swift, M. R., Pham, V. N., Castranova, D., Bell, K., Poole, R. J. and Weinstein, B. M. (2014). SoxF factors and Notch regulate nr2f2 gene expression during venous differentiation in zebrafish. *Dev. Biol.* **390**, 116-125.

Tian, X.-L., Kadaba, R., You, S.-A., Liu, M., Timur, A. A., Yang, L., Chen, Q., Szafranski, P., Rao, S., Wu, L. et al. (2004). Identification of an angiogenic factor that when mutated causes susceptibility to Klippel-Trenaunay syndrome. *Nature* **427**, 640-645.

Wiley, D. M., Kim, J.-D., Hao, J., Hong, C. C., Bautch, V. L. and Jin, S.-W. (2011). Distinct signalling pathways regulate sprouting angiogenesis from the dorsal aorta and the axial vein. *Nat. Cell Biol.* **13**, 686-692.

Wythe, J. D., Dang, L. T. H., Devine, W. P., Boudreau, E., Artap, S. T., He, D., Schachterle, W., Stainier, D. Y. R., Oettgen, P., Black, B. L. et al. (2013). ETS factors regulate Vegf-dependent arterial specification. *Dev. Cell* **26**, 45-58.

Yamamizu, K., Matsunaga, T., Uosaki, H., Fukushima, H., Katayama, S., Hiraoka-Kanie, M., Mitani, K. and Yamashita, J. K. (2010). Convergence of Notch and β-catenin signaling induces arterial fate in vascular progenitors. *J. Cell Biol.* **189**, 325-338.

You, L.-R., Lin, F.-J., Lee, C. T., DeMayo, F. J., Tsai, M.-J. and Tsai, S. Y. (2005). Suppression of Notch signalling by the COUP-TFII transcription factor regulates vein identity. *Nature* **435**, 98-104.

Zhang, J., Fukuhara, S., Sako, K., Takenouchi, T., Kitani, H., Kume, T., Koh, G. Y. and Mochizuki, N. (2011). Angiopoietin-1/Tie2 signal augments basal Notch signal controlling vascular quiescence by inducing delta-like 4 expression through AKT-mediated activation of β-catenin. *J. Biol. Chem.* **286**, 8055-8066.

Supplementary Materials and Methods

Plasmids

A cDNA fragment encoding β-catenin binding domain of human TCF4E (amino acid 1-314) was amplified by PCR using pCMXGAL4/hTCF4E vector, a gift from A. Kikuchi (Osaka University, Japan), as a template, and subcloned into pCMV-BD vector (Stratagene) to construct pCMV-Gal4db-TΔC plasmid that encodes the β-catenin binding domain of TCF4 fused to the DNA binding domain of Gal4 (Gal4db-TΔC). The pCMV-Gal4db-TΔC (D16A) plasmid encoding Gal4db-TΔC mutant in which Asp-16 of TCF4E was replaced with Ala was generated using QuickChange Site-directed mutagenesis kit (Stratagene).

The Tol2 vector system was kindly provided by K. Kawakami (National Institute of Genetics, Japan) (Kawakami et al., 2004; Urasaki et al., 2006). The pTol2-fli1 vector was constructed by removing a cDNA fragment containing GFP and Gateway cassette from the pTolfli1epEGFPDest plasmid, a gift from N. Lawson (University of Massachusetts Medical School, USA) (Lawson and Weinstein, 2002). To generate the pTolflk1 plasmid, the *fli1* enhancer/promoter was removed from the pTolfli1 vector, and replaced with the *flk1* promoter, a gift from D.Y. Stainier (Max Planck Institute). The cDNA encoding Gal4db-TΔC followed by 2A peptide and mCherry was subcloned into pTol2-fli1 vector to generate the pTol2-fli1:Gal4db-TΔC-2A-mC plasmid. The pTol1 vector was constructed by modifying pDon122 vector (COSMO BIO CO., LTD). To generate the pTol1-UAS and pTol2-UAS plasmids, the upstream activating sequence (UAS) derived from pBluescript II-UAS:GFP vector, a gift from M. Hibi (Nagoya University, Japan), was inserted into pTol1 and pTol2 vectors, respectively.

cDNA fragments encoding zebrafish *tcf3*, *dkk1*, *noggin3*, *bmp2b*, *aggf1*, *nr2f2*, *flt4*, *fli1a*, *axin1* and *wnt3a* were amplified from cDNAs library derived from zebrafish embryos by PCR and cloned into pCR4 Blunt TOPO vector (Invitrogen). The pTol1-UAS:TΔN-GFP plasmid was constructed by inserting a cDNA fragment that encodes Tcf3 lacking β-catenin binding domain (amino acid 55-561) followed by GFP (TΔN-GFP) into pTol1-UAS vector. An oligonucleotide encoding nuclear localization signal (NLS) derived from SV40 (PKKKRKV) was inserted into pEGFP-C1 and pmCherry-C1 vectors (Clontech, Takara Bio Inc.) to generate the plasmids expressing NLS-tagged GFP (NLS-GFP) and NLS-tagged mCherry (NLS-mC), respectively. The NLS-GFP cDNA was subcloned into the pTol2-UAS vector to construct the pTol2-UAS:NLS-GFP plasmid. An oligonucleotide encoding the myristoylation (Myr) signal derived from Lyn kinase was subcloned into pmCherry-N1 vector (Clontech, Takara Bio Inc.) to construct the plasmid encoding Myr signal-tagged mCherry (Myr-mC). The pTol2-fli1:Myr-mC plasmid was constructed by inserting Myr-mC cDNA into the pTol2-fli1 vector. An oligonucleotide encoding NLS derived from SV40 was inserted into the EcoRI/XhoI sites of a pcDNA3-td-EosFP vector (Molecular Biotechnology) to generate the plasmid encoding NLS-tagged tandem dimer Eos fluorescence protein (NLS-Eos). To construct pTolflk1-NLS-Eos vector, the NLS-Eos cDNA was subcloned into the pTolflk1 vector.

The DNA sequence of zebrafish heat shock protein 70 promoter was derived from pHSP70/4 EGFP plasmid (provided by J. Kuwada, University of Michigan, USA) (Halloran et al., 2000), and subcloned into the pTol2, namely the pTol2-hsp70l plasmid. The pTol2-hsp70l:dkk1-FLAG and the pTol2-hsp70l:wnt3a-FLAG plasmids were generated by inserting a cDNA fragment encoding C-terminally FLAG-tagged dkk1 and

that encoding C-terminally FLAG-tagged wnt3a into the pTol2-hsp70l plasmid, respectively.

The DNA sequence encoding zebrafish cardiac myosin light chain 2 (cmlc2) promoter was cloned by PCR using zebrafish genomic DNA as a template, and inserted into the pTol2 vector to construct the pTol2-cmlc2. The pTol2-cmlc2:NLS-mC plasmid was constructed by inserting the NLS-mC cDNA into the pTol2-cmlc2. Then, the chicken β-globin insulator (HS4) derived from pJC13-1 vector, a gift from G. Felsenfeld (National Institute of Health, USA) (Chung et al., 1993), and the zebrafish heat shock protein 70 promoter were sequentially subcloned into pTol2-cmlc2:NLS-mC to construct the pTol2-cmlc2:NLS-mC-HS4-hsp70l plasmid. The cDNA fragments expressing FLAG-tagged noggin3 and FLAG-tagged bmp2b, in which FLAG tag was inserted immediately after their signal sequence, were subcloned into the pTol2-cmlc2:NLS-mC-HS4-hsp70l vector to generate the pTol2-cmlc2:NLS-mC-HS4-hsp70l:noggin3-FLAG (hsp70l:noggin3-FLAG) and the pTol2-cmlc2:NLS-mC-HS4-hsp70l:FLAG-bmp2b-FLAG (hsp70l:bmp2b-FLAG) plasmids, respectively.

A cDNA fragment encoding human AGGF1 was amplified by PCR from human heart cDNAs, and subcloed into pEGFP-N1 vector to generate pEGFP-N1-AGGF1. The pmCherry-N1-Aggf1 was constructed by inserting the zebrafish aggf1 cDNA into pmCherry-N1 vector. The aggf1-mCherry cDNA was subcloned into pCS2+ vector, namely pCS2-Aggf1-mCherry.

The expression vectors encoding wild type and constitutive active β-catenin have already been reported (Zhang et al., 2011). To construct pCMV-Gal4-β-catenin that encodes β-catenin N-terminally fused to DNA binding domain of Gal4, the β-catenin

cDNA was subcloned into pCMV-BD vector. The pCS2+Gal4FF vector that expresses an engineered transcriptional activator consisting of the DNA-binding domain of Gal4 fused to two transcription activation modules from VP16 (Gal4-VP16) was kindly provided by M. Hibi (Nagoya University, Japan). pFR-Luc plasmid was purchased from Stratagene. pRL-SV40, pRL-TK, TOPflash and FOPflash vectors were obtained from Addgene.

To construct the pTol2-E1b-UAS-E1b vector, the UAS flanked by E1b minimal promoters on both sides was inserted into the pTol2 vector. A cDNA encoding NLS-GFP together with polyA signal and that encoding FLAG-tagged axin1 with polyA signal were sequentially subcloned into the pTol2-E1b-UAS-E1b vector to construct the pTol2-UAS:NLS-GFP,Axin plasmid (UAS:NLS-GFP,Axin), which drives expression of both NLS-GFP and FLAG-tagged Axin simultaneously in a Gal4-dependent manner.

Transgenic zebrafish lines

Tol1 and Tol2 transposase mRNAs were *in vitro* transcribed with SP6 RNA polymerase from NotI-linearised pCS-TP vector using the mMESSAGE mMACHINE kit (Ambion). To generate the *Tg(fli1:Gal4db-TΔC-2A-mC)*, *Tg(fli1:Myr-mC)*, *Tg(UAS:TΔN-GFP)*, *Tg(UAS:NLS-GFP)*, *Tg(flk1:NLS-Eos)* and *Tg(hsp70l:dkk1-FLAG)* zebrafish lines, the corresponding Tol1- or Tol2-based plasmid DNAs (25 ng) were microinjected along with Tol1 or Tol2 transposase RNA (25 ng) into one-cell stage embryos of wild type strain, AB. To establish the *Tg(fli1:Gal4db-TΔC-2A-mC)*, *Tg(fli1:Myr-mC)* and *Tg(flk1:NLS-Eos)* fish lines, the embryos showing transient expression of mCherry or Eos fluorescence in the vasculature were selected, raised to adulthood, and crossed with wild type AB to identify germline transmitting founder fishes. To develop the

Tg(UAS:TΔN-GFP) and *Tg(UAS:NLS-GFP)* Tg lines, the fish carrying the corresponding genes were first screened by genomic PCR, and confirmed by crossing with *Tg(fli1:Gal4FF)* zebrafish to check the transgene expression. To generate the *Tg(hsp70l:dkk1-FLAG)* fish line, all embryos were raised to adulthood, and subjected to genomic PCR screening. Embryos obtained from crossing the genomic PCR-positive fish with wild type AB were heat-shocked to check the transgene expression. The *Tg(flt1:mC)* zebrafish line was generated as previously reported (Bussmann et al., 2010).

Tg(fli1:GFP) fish were provided by N. Lawson (University Massachusetts Medical School, USA) (Lawson and Weinstein, 2002). *Tg(UAS:GFP)* and *Tg(UAS:RFP)* fish lines were kindly provided by K. Kawakami (National Institute of Genetics, Japan) (Asakawa et al., 2008). *Tg(fli1:Gal4FF)* fish line was a gift from M. Affolter (University of Basel, Switzerland) (Totong et al., 2011; Zygmunt et al., 2011). *Tg(hsp70l:dkk1-GFP)* fish were obtained from the Zebrafish International Resource Center (University of Oregon, OR, USA).

Mounting of zebrafish embryos

Pigmentation of embryos was inhibited by 1-phenyl-2-thiourea (PTU) (Sigma-Aldrich). Embryos were dechorionated, anesthetised in 0.016% tricaine (Sigma-Aldrich) in E3 embryo medium, and mounted in 1% low-melting agarose dissolved in E3 medium poured on a 35-mm-diameter glass-base dish (Asahi Techno Glass). The mounted embryos were submerged in E3 medium supplemented with 0.016% tricaine and 0.2 mM PTU.

Quantitative analyses of fluorescence, CV defects and ectopic vessel formation

To quantify the β-catenin transcriptional activity in CVP in the Figures 1D, 3B, 3D, 5D, 5F, S3G and S6E, 3D-renderd confocal stack fluorescence images of GFP and mCherry in the caudal regions of *Tg(fli1:Gal4db-TΔC-2A-mC);(UAS:GFP);(fli1:Myr-mC)* fish embryos at 36 hpf were acquired using confocal microscopy. The mCherry fluorescence-marked CVP on the 3D-images was manually cropped using Volocity software. Then, the volume of the cropped areas and the total GFP fluorescence intensity within the areas were calculated. The β-catenin transcriptional activity in the CVP was determined by dividing the total GFP fluorescence intensity by the volume of CVP.

To quantify the defective CV formation in the Figures 2D, 4D, 6I, S6B and S8F, the CV of *Tg(fli1:Myr-mC)* or *Tg(fli1:GFP)* embryos at 48 hpf were analyzed and classified into two groups: mild group and severe group. In the Figures 2D, 4D and S6B, the embryos with mild phenotype exhibited no blood circulation in the CV, whereas those with severe phenotype lacked CV. In the Figures 6I and S8F, the embryos with the mild phenotype lacked the CV, but developed the CVP, whereas those with the severe phenotypes exhibited lack of the CV and defective CVP. Frequency of mild and severe phenotypes is expressed as percentage relative to the total number of analyzed embryos.

To quantify formation of ectopic venous vessels in Bmp2b-overexpressing embryos in Figure 4E, the *Tg(fli1:GFP)* embryos were analyzed at 48 hpf. The areas covered by ectopic venous vessels within 11 somites in the caudal regions were measured using Volocity software.

RNA-seq analyses

Using total RNA purified from β-catenin (+) ECs and β-catenin (-) ECs, reverse transcription and cDNA library preparation were performed with SMARTer Ultra Low RNA Kit (Clontech). cDNA was fragmented with a Covaris S220 instrument (Covaris). Subsequently, the sample was end-repaired, dA-tailed, adaptor ligated, and then subjected to PCR by using the NEBNext® DNA Library Preparation and NEBNext Multiplex oligos For Illumina. The sample was sequenced by using MiSeq (Illumina) to generate pair-end 150-bp reads.

Raw reads were mapped to Zebrafish genome (DanRer7). Expression levels were measured by calculating RPKM (reads per kilobase per million sequenced reads), and normalised TMM (Trimmed Mean of M-values) method by using Avadis NGS software (Strand Life Sciences).

TUNEL assay

EC apoptosis was analyzed by TUNEL assay. *Tg(UAS:NLS-GFP);(fli1:Gal4FF)* or *Tg(UAS:TΔN-GFP);(fli1:Gal4FF)* embryos at 32 hpf were dechorinated, fixed with 4% paraformaldehyde (PFA) at 4 °C overnight, and dehydrated with methanol (MeOH) at -20 °C. After gradual hydration, the embryos were permeabilised with 5 μg/ml proteinase K, refixed with 4% PFA, and washed three times with PBS-T. Then, apoptotic cells were stained by using In Situ Cell Death Detection Kit, TMR red (Roche). To quantify the EC apoptosis, we counted TUNEL-positive cells among the GFP-positive ECs.

Heat shock and chemical treatment

Tg(hsp70l:dkk1-GFP) and *Tg(hsp70l:dkk1-FLAG)* embryos were heat shocked at either 12 or 24 hpf for 1 h at 39 °C. *Tg(hsp70l:dkk1-GFP)* embryos were identified by the expression of GFP. *Tg(hsp70l:dkk1-FLAG)* embryos were identified based on the appearance of defective caudal fin formation as described in Figure S3, and confirmed by genomic PCR after the analyses. To ubiquitously express wnt3a-FLAG, the *Tg(fli1:Gal4db-TΔC-2A-mC);(UAS:GFP);(fli1:Myr-mC)* embryos were injected with 25 ng pTol2-hsp70l:wnt3a-FLAG plasmid along with Tol2 transposase RNA (25 ng), and heat-shocked at 22 hpf for 1 h at 39 °C. To ubiquitously express noggin3-FLAG and bmp2b-FLAG, the *Tg(fli1:Gal4db-TΔC-2A-mC);(UAS:GFP);(fli1:Myr-mC)* embryos were injected with 25 ng pTol2-cmlc2:NLS-mC-HS4-hsp70l:noggin3-FLAG (hsp70l:noggin3-FLAG) and 25 ng pTol2-cmlc2:NLS-mC-HS4-hsp70l:bmp2b-FLAG (hsp70l:bmp2b-FLAG) plasmids along with Tol2 transposase RNA (25 ng), and heat-shocked at 22 hpf for 2 h and at 24 hpf for 30 min at 39 °C, respectively. The embryos carrying the corresponding genes were selected by the expression of mCherry in cardiac myocytes.

Tg(fli1:Gal4db-TΔC-2A-mC);(UAS:GFP);(fli1:Myr-mC) embryos were dechorinated, and incubated from 24 to 33 or 48 hpf and from 15 to 36 hpf in the E3 medium containing 1 or 3 μM BIO, a glycogen synthase kinase 3 inhibitor (6-bromoindirubin-3'-oxime, EMD Biosciences) and 10 μM IWR-1, an axin-stabilising compound (Calbiochem), respectively. As a control, the embryos were also incubated in the E3 solution containing DMSO. *Tg(flk1:NLS-Eos)* embryos were incubated in the E3 medium containing either DMSO or 1.5 μM Ki 8457, an inhibitor for Vegf-A receptor (Tocris).

Cell culture, transfection and luciferase reporter assay

HEK 293 and HEK 293T cells and human umbilical vein ECs were cultured and transfected as described previously (Fukuhara et al., 2008). To investigate whether β-catenin stimulates transcriptional activity of Gal4db-TΔC, HEK 293 cells were transfected with either pCMV-Gal4db-TΔC or pCMV-Gal4db-TΔC (D16A) vector together with pFR-Luc and pRL-TK that encode firefly and renilla luciferase under the control of five tandem repeats of Gal4 binding sites and herpes simplex virus thymidine kinase promoter, respectively. The transfection mixture also included either the expression plasmid encoding wild type β-catenin or the empty vector. The total amount of plasmid DNA was adjusted with empty vector. The cells were lysed using passive lysis buffer (Promega) 16 h after the transfection. To examine the effect of BIO, the cells were stimulated with 5 μM BIO for 16 h. The luciferase activities in cell extracts were determined by using a Dual-Luciferase assay system (Promega). To normalize the levels of the experimental reporter activity, firefly luciferase activity are divided by renilla luciferase activity for each sample.

To examine the effect of Aggf1 on β-catenin transcriptional activity, the cells were transfected with either TOPflash or FOPflash plasmid together with pRL-SV40 vector. The transfection mixtures also included the expression plasmids as described in the figure legends. The luciferase activities in the cells were measured 24 h after the transfection. To normalize the levels of the experimental reporter activity, firefly luciferase activity were divided by renilla luciferase activity for each sample. The levels of β-catenin/Tcf-dependent transcription were indicated by the value of TOPflash luciferase activity divided by that of FOPflash activity. The cells were also transfected

with the expression plasmid encoding either Gal4-β-catenin or Gal4-VP16 together with pEGFP-N1-Aggf1 or the empty plasmid, and lysed 24 h after the transfection.

Injections of morpholino oligonucleotide (MO) and mRNA

For morpholino oligonucleotide (MO)-mediated gene knockdown, embryos were injected at the one-cell or two-cell stage with control MO (Gene Tools), 2.5 ng of *aggf1* splicing MO (*aggf1* MO1), 10 ng of *aggf1* translation blocking MO (*aggf1* MO2), 4 ng of *nr2f2* splicing MO (*nr2f2* E1I1 MO), 2 ng of *nr2f2* translation blocking MO (*nr2f2* ATG MO) (Gene Tools). To suppress the cell death induced by MO off-targeting, *p53* MO was co-injected 1.5-fold (w/w) to the other MO used, as previously reported (Robu et al., 2007). The sequences for the already-validated MOs used in this study are: *aggf1* MO1, 5'-GCCCTGCTCACCTGCTGTCGGAGAT-3' (Chen et al., 2013); *aggf1* MO2, 5′-CGCATCAATAGGGAGCAACCGCGAT-3′ (Chen et al., 2013); *nr2f2* E1I1 MO, 5′-ACAAAAATCCGAATACCTTCCCGTC-3′ (Aranguren et al., 2011); *nr2f2* ATG MO, 5′-AGCCTCTCCACACTACCATTGCCAT-3′ (Aranguren et al., 2011).

aggf1-mCherry mRNA was *in vitro* transcribed with SP6 RNA polymerase from pCS2-Aggf1-mCherry vector using the mMESSAGE mMACHINE kit (Ambion). To ubiquitously express Aggf1-mCherry, 200 pg of *aggf1-mcherry* mRNA was injected into one cell stage of *Tg(fli1:Gal4db-TΔC-2A-mC);(UAS:GFP);(fli1:Myr-mC)* embryo.

Genotyping

For the genotyping of the zebrafish Tg lines, genomic PCR were performed using the following primer sets: for *Tg(UAS:TΔN-GFP)* and *Tg(UAS:NLS-GFP)*, 5'-GAAGCAGCACGACTTCTTCAAGTCC-3' and

5’-CCTTGATGCCGTTCTTCTGCTTGTC-3’; for *Tg(hsp70l:dkk1-FLAG)*,

5’-ATAATGAAACAATTGCACCGATAA-3’ and

5’-GAAGTTCAGACTGTCCAAAAGTGA-3’.

Real-time reverse transcription PCR

Real-time reverse transcription PCR was performed as previously described (Fukuhara et al., 2008).

Kashiwada_Supplementary Figure S1

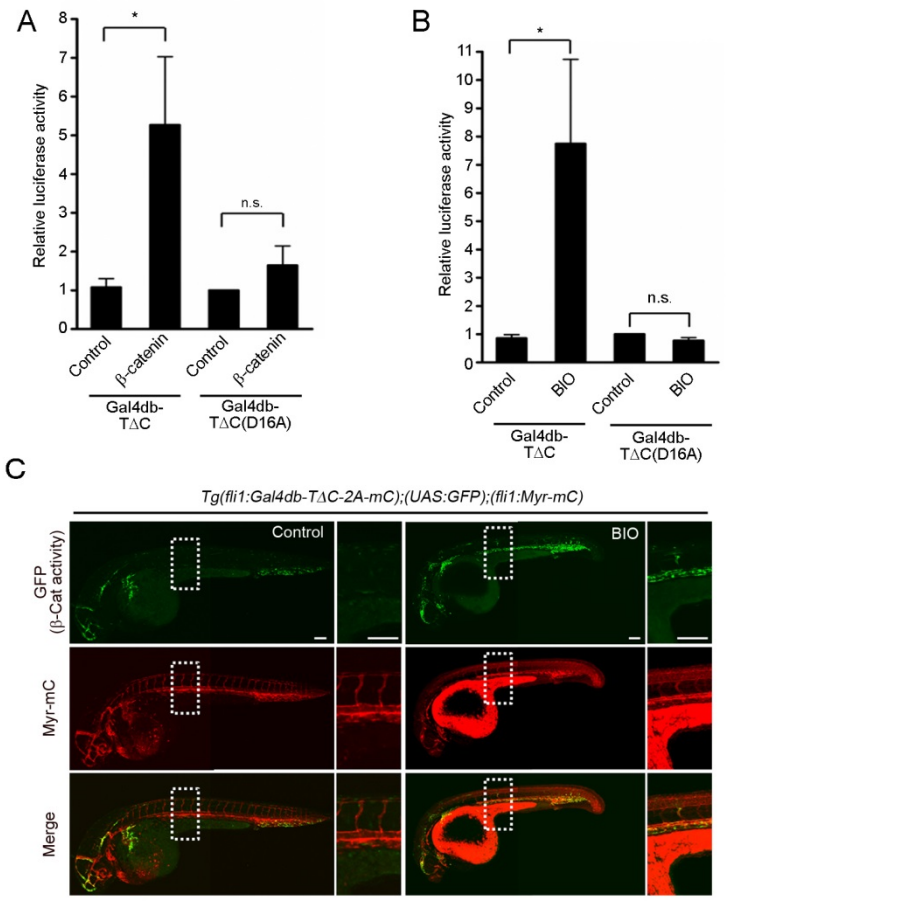

Supplementary Figure S1. Reporter gene expression driven by Gal4db-TΔC reflects transcriptional activity of β-catenin. (A) Relative luciferase activity in HEK 293T cells transfected with UAS-luciferase reporter and the plasmid encoding either Gal4db-TΔC or its mutant (Gal4db-TΔC(D16A)) that lacks the ability to bind β-catenin together with the empty vector (Control) or that encoding β-catenin. Data are expressed relative to that observed in the empty vector-transfected cells that express Gal4db-TΔC (D16A), and shown as mean ± s.e.m. of four independent experiments. (B) Relative luciferase activity in 5 μM BIO-stimulated HEK 293T cells transfected with UAS-luciferase reporter and the plasmid encoding either Gal4db-TΔC or Gal4db-TΔC (D16A). The cells were stimulated with vehicle (Control) or BIO for 16 h. Data are expressed relative to that observed in the vehicle-treated cells that express Gal4db-TΔC (D16A), and shown as mean ± s.e.m. of three independent experiments. (C) 3D-rendered confocal stack fluorescence images of the

Tg(fli1:Gal4db-TΔC-2A-mC);(UAS:GFP);(fli1:Myr-mC) embryos treated with vehicle (Control) or 3 μM BIO, a glycogen synthase kinase 3 inhibitor, from 24 to 33 hours post-fertilization (hpf). Top, GFP images (β-Cat activity); middle, mCherry images (Myr-mC); bottom, the merged images (Merge). The images are composites of two images, since it was not possible to capture the whole animal at sufficiently high resolution in a single field of view. The boxed areas are enlarged on the right side of the original images. *p<0.05. n.s., no significance.

Kashiwada_Supplementary Figure S2

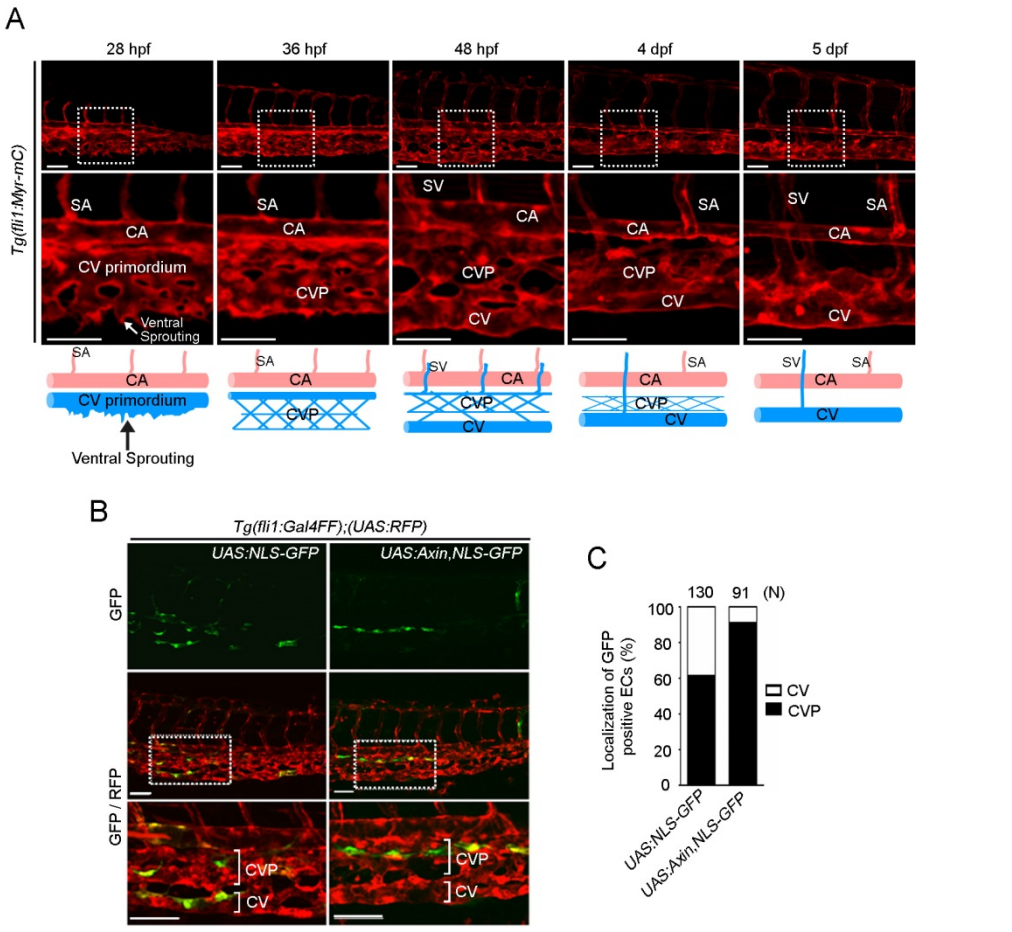

Supplementary Figure S2. The development of the caudal vein (CV). (A) Confocal images of caudal regions of *Tg(fli1:Myr-mC)* embryos at the developmental stages indicated at the top. The boxed areas are enlarged beneath the original images. Schematic representations of the caudal vessel structures are shown at the bottom. (B) Confocal images of the caudal regions of the 48 hpf *Tg(fli1:Gal4FF);(UAS:RFP)* embryos injected with *UAS:NLS-GFP* Tol2 plasmid or *UAS:Axin,NLS-GFP* Tol2 plasmid, which drives the expression of Axin and NLS-GFP simultaneously. GFP images and the merged images of GFP (green) and RFP (red) are shown in the top and middle rows, respectively. The boxed areas in the merged images are enlarged in the bottom row. (C) Percentages of GFP-expressing cells in the CV and CVP as observed in B were quantified. The number of analyzed embryos is indicated on the top. CA, caudal artery; CV, caudal vein; CVP, caudal vein plexus; SA, segmental artery; SV, segmental vein.

Kashiwada_Supplementary Figure S3

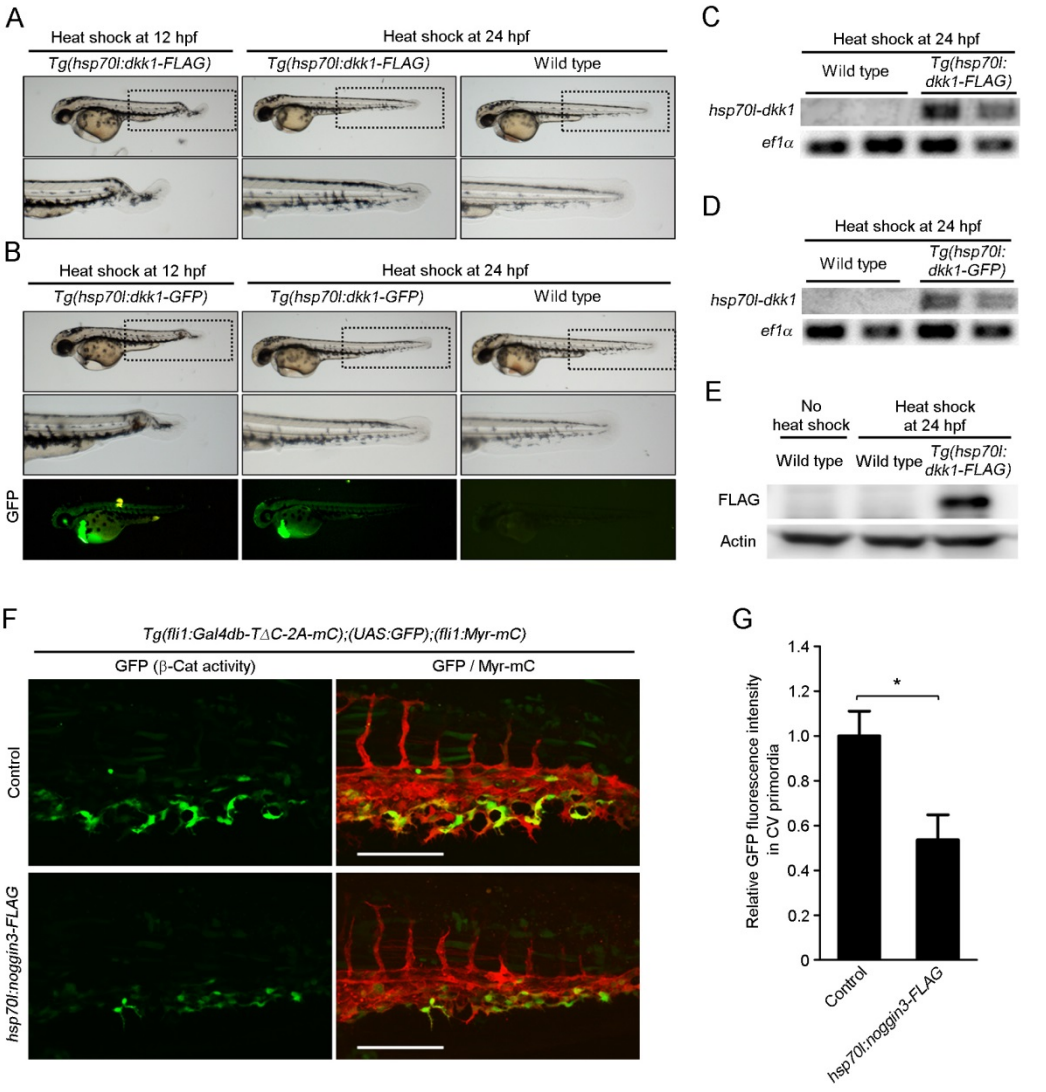

Supplementary Figure S3. Wnt signaling is suppressed by heat shock promoter-driven expression of dkk1. (A) Lateral view of wild type sibling and *Tg(hsp70l:dkk1-FLAG)* embryos heat-shocked at either 12 or 24 hpf as indicated at the top. The boxed areas are enlarged beneath the original images. (B) Lateral view of wild type sibling and *Tg(hsp70l:dkk1-GFP)* embryos heat-shocked at either 12 or 24 hpf as indicated at the top. The boxed areas are enlarged beneath the original images. GFP fluorescence images are shown at the bottom. (C, D) Genomic PCR analysis of wild type sibling, *Tg(hsp70l:dkk1-FLAG)* (C) and *Tg(hsp70l:dkk1-GFP)* (D) zebrafish

embryos were performed using primer sets to amplify the DNA fragment that contains *heat shock promoter* and *dkk1* and to amplify the *ef1α* gene. (E) Western blot analysis of lysates from heat-shocked wild type and *Tg(hsp70l:dkk1-Flag)* embryos with anti-FLAG and anti-βactin (Actin) antibodies. (F) Confocal stack fluorescence images of the 28 hpf *Tg(fli1:Gal4db-TΔC-2A-mC);(UAS:GFP);(fli1:Myr-mC)* embryos injected without (Control) or with *hsp70l:noggin3-FLAG* plasmid and heat-shocked at 24 hpf for 1h. GFP images (β-Cat activity); right, the merged (GFP/Myr-mC) of GFP (green) and mCherry (red) images. Scale bars, 100 μm. (G) Fluorescence intensities of GFP in the CV primordia and the ECs that sprouted from the CV primordia, as observed in F, were expressed as relative values to that observed in the control embryos. Data are shown as means ± s.e.m. (Control n=8, *hsp70l:noggin3-FLAG* n=5).

Kashiwada_Supplementary Figure S4

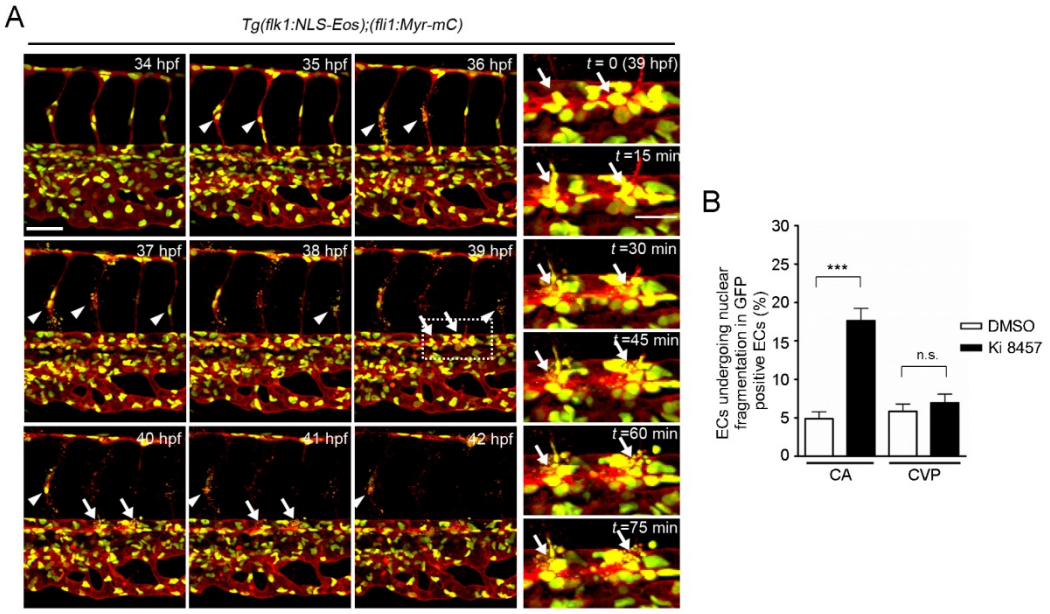

Supplementary Figure S4. Vegf-A promotes EC survival in the caudal artery (CA). (A) *Tg(flk1:NLS-Eos);(fli1:Myr-mC)* embryos were treated with 1.5 μM Ki 8457, an inhibitor for Vegf-A receptor, from 30 hpf, and subjected to time-lapse confocal imaging from 34 hpf to 42 hpf. The merged images of Eos (green) and mCherry (red) at every hour starting from 34 to 42 hpf are shown. The enlarged image of boxed area in the image at 39 hpf and its subsequent time-lapse images are shown at the right column. The elapsed time (min) is indicated at the top of each image. Arrowheads and arrows indicate the ECs undergoing nuclear fragmentation in the ISV and CA, respectively. Scale bars, 50 μm. (B) Percentage of DMSO-treated or Ki 8457-treated NLS-Eos-expressing ECs that undergo nuclear fragmentation in the CA and CVP between 34-42 hpf. Data are expressed as a percentage relative to the total number of NLS-Eos-expressing ECs, and shown as mean ± s.e.m. (DMSO n=6, Ki 8457 n=6). ***p<0.01. n.s., no significance.

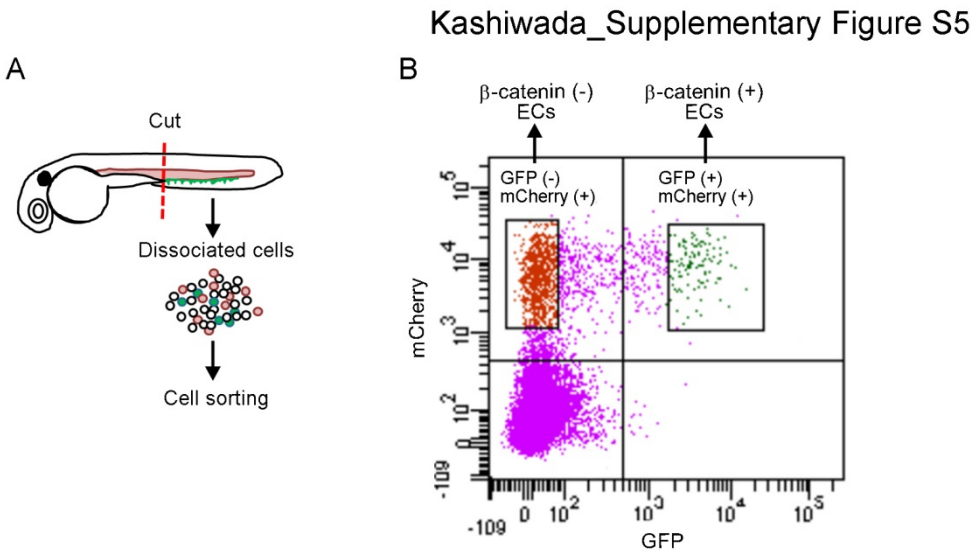

Supplementary Figure S5. Isolation of β-catenin (+) ECs from the caudal regions of EC-specific β-catenin reporter zebrafish. (A) Schematic representation of the purification of the β-catenin (+) and β-catenin (-) ECs for RNA-seq analyses. (B) To identify the genes that are upregulated and downregulated in β-catenin (+) ECs, GFP-positive and mCherry-positive ECs (β-catenin (+) ECs) and GFP-negative and mCherry-positive ECs (β-catenin (-) ECs) were isolated from the caudal parts of *Tg(fli1:Gal4db-TΔC-2A-mC);(UAS:GFP);(fli1:Myr-mC)* embryos using flow cytometry.

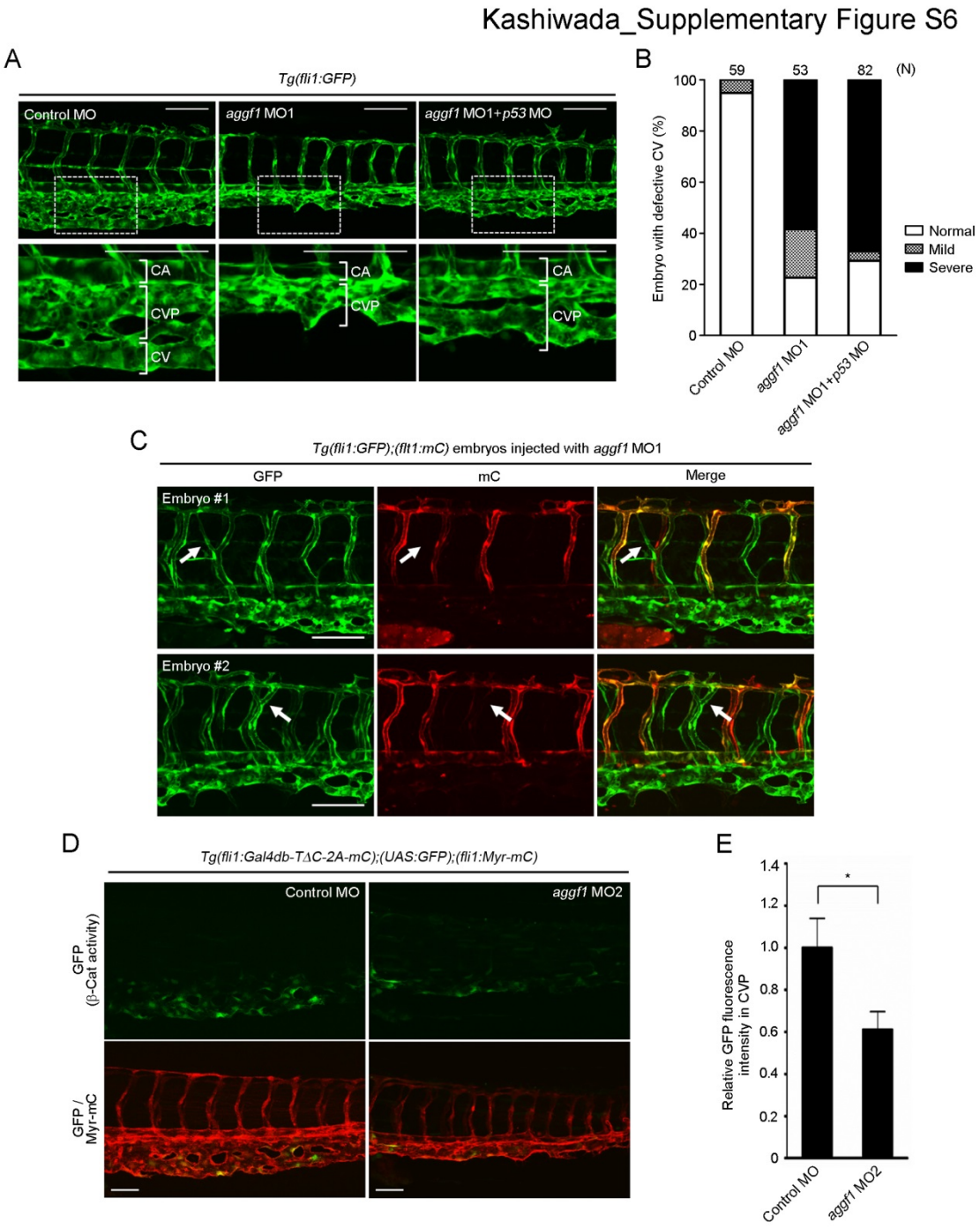

Supplementary Figure S6. Aggf1 stimulates β-catenin-dependent transcription in ECs to develop the CV. (A) Confocal stack images of the caudal regions of the 48 hpf *Tg(fli1:GFP)* embryos injected with control MO (left column), *aggf1* MO1 (middle column) or a mixture of *aggf1* MO1 and *p53* MO (right column). The boxed areas are

enlarged at the bottom. CA, caudal artery; CV, caudal vein; CVP, caudal vein plexus. (B) The CV phenotypes observed in A were quantified, as in Figure 2D. (C) Confocal images of caudal regions of 48 hpf *Tg(fli1:GFP);(flt1:mC)* embryos injected with *aggf1* MO1. Two representative embryos are shown (Embryo #1 and Embryo #2). Left, GFP images; middle, mCherry images (mC); right, the merged images (Merge). mCherry fluorescence marks the arterial ECs. Arrows indicate defective ISVs. Note that formation of venous ISVs was mainly affected by depletion of Aggf1. (D) Confocal images of caudal regions of 36 hpf *Tg(fli1:Gal4db-TΔC-2A-mC);(UAS:GFP);(fli1:Myr-mC)* embryos injected with either control MO or *aggf1* MO2. Upper, GFP images (β-Cat activity); lower, merged images of GFP (green) and mCherry (red) (GFP/Myr-mC). (E) Fluorescence intensity of GFP in the caudal vein plexus (CVP) as observed in D was quantified, and expressed as a relative value to that observed in the control MO-transfected embryos. Data are shown as mean ± s.e.m. (Control MO n=14, *aggf1* MO2 n=15). **p*<0.05. Scale bars, 100 μm (A, C) and 50 μm (D).

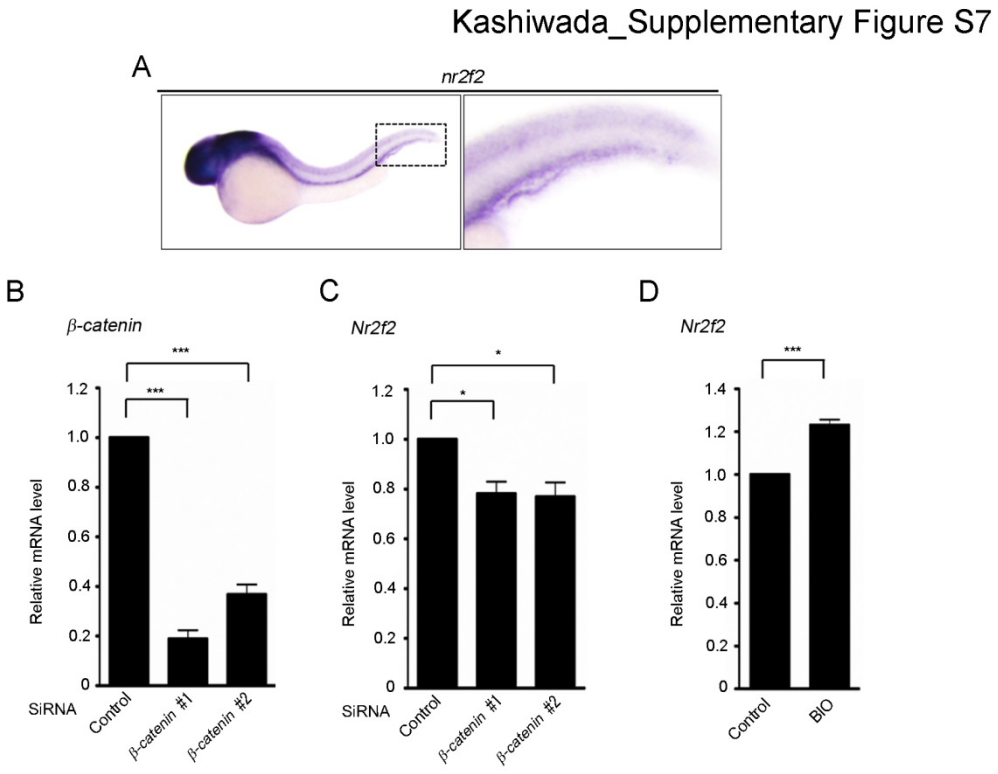

Supplementary Figure S7. β-catenin regulates expression of *NR2F2*. (A) Expression pattern of *nr2f2* mRNA in zebrafish embryos at 48 hpf, as detected by whole-mount *in situ* hybridization. The boxed area is enlarged at the right. (B, C) Total RNA was extracted from human umbilical vein ECs transfected with either control siRNA or two independent siRNAs targeting *β-catenin* (#1 and #2), and subjected to real-time RT-PCR analysis to determine the expression levels of *β-catenin* (B) and *NR2F2* (C) mRNAs. Bar graphs show relative mRNA levels of *β-catenin* and *NR2F2* normalized to that of *GAPDH*. Data are expressed relative to that in control siRNA-transfected cells, and shown as mean ± s.e.m. (n=4). (D) Total RNA was extracted from human umbilical vein ECs stimulated with vehicle (Control) or 2 μM BIO for 24 h, and subjected to real-time RT-PCR analysis to determine the expression levels of *NR2F2* mRNA, as in B. Data are expressed relative to that in control cells, and shown as mean ± s.e.m. (n=4). **p*<0.05, ***p*<0.01, ****p*<0.001.

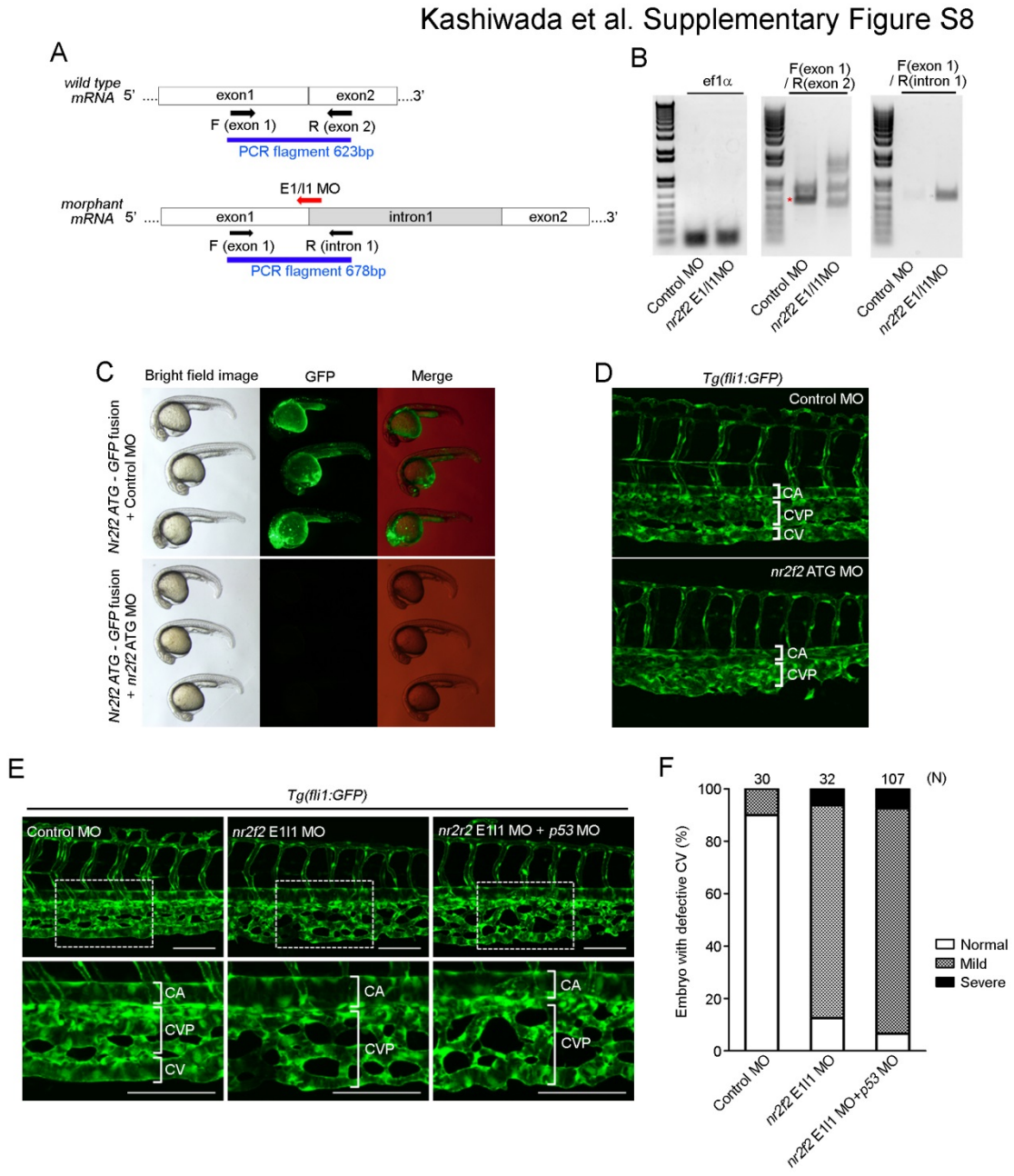

Supplementary Figure S8. Nr2f2 is required for CV formation. (A) *nr2f2* E1/I1 MO (red arrow) is a splice-blocking MO that targets the boundary between exon 1 and intron 1. Schematic diagrams of normally-spliced mRNA (upper) and aberrantly-spliced mRNA produced in *nr2f2* E1/I1 MO-injected embryos (lower). (B) RT-PCR analyses of RNAs extracted from the zebrafish embryos injected from control MO or *nr2f2* E1/I1 MO were performed using two sets of PCR primers as indicated in A (F(exon 1)/R(exon

2); F(exon 1)/R(intron 1)) as well as an *ef1a* primer. PCR using a primer set of F(exon 1)/R(exon 2) amplified the 623-bp fragment (single asterisk) corresponding to normally-spliced *nr2f2* mRNA in control MO-injected embryos, but not in those injected with *nr2f2* E1I1 MO. In contrast, PCR using a primer set of F(exon 1)/R(intron 1) amplified the 678-bp fragment (double asterisks) that contains partial sequence of exon 1 and intron 1 only in *nr2f2* E1I1-injected embryos. These results suggest that *nr2f2* E1/I1 MO efficiently blocks splicing of exon 1 and 2, leading to inclusion of intron 1 and the creation of premature stop codon. (C) Bright field images (left column), GFP images (middle column) and the merged images (right column) of 24 hpf embryos injected with mRNA encoding amino acids 1-27 of Nr2f2 C-terminally tagged with GFP (Nr2f2 ATG-GFP fusion) together with control MO (upper) or *nr2f2* ATG MO (lower). Note that injection of *nr2f2* ATG MO efficiently suppressed expression of Nr2f2 ATG-GFP fusion protein. (D) Confocal stack images of the caudal regions of the 48 hpf *Tg(fli1:GFP)* embryos injected with control MO or *nr2f2* ATG MO. (E) Confocal stack images of the caudal regions of the 48 hpf *Tg(fli1:GFP)* embryos injected with control MO (left column), *nr2f2* E1I1 MO (middle column) or a mixture of *nr2f2* E1I1 MO and *p53* MO (right column). The boxed areas are enlarged at the bottom. (F) The CV phenotypes observed in E were classified and quantified, as in Figure 6H and 6I. CA, caudal artery; CV, caudal vein; CVP, caudal vein plexus. Scale bars, 100 μm.

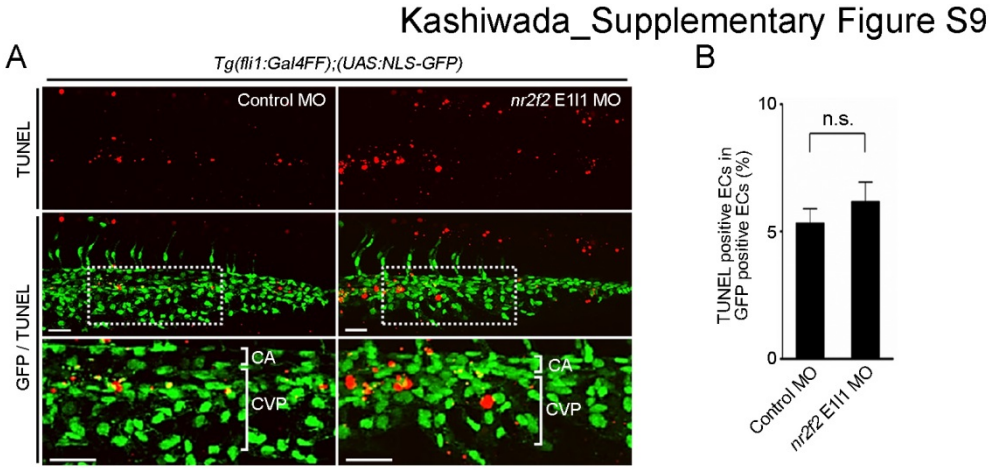

Supplementary Figure S9. Nr2f2 is not involved in survival of venous ECs during CV formation. (A) Confocal stack fluorescence images of the 32 hpf *Tg(fli1:Gal4FF);(UAS:NLS-GFP)* embryos injected with either control MO or *nr2f2* E1I1 MO and subjected to TUNEL staining. Top, TUNEL signal; middle, the merged images (GFP/TUNEL) of GFP (green) and TUNEL (red); bottom, the enlarged images of boxed areas. Scale bars, 50 µm. (B) Percentage of TUNEL-positive ECs among the NLS-GFP-expressing ECs in the CVP of the embryos injected with control MO or *nr2f2* E1I1 MO as observed in A. n.s., no significance.

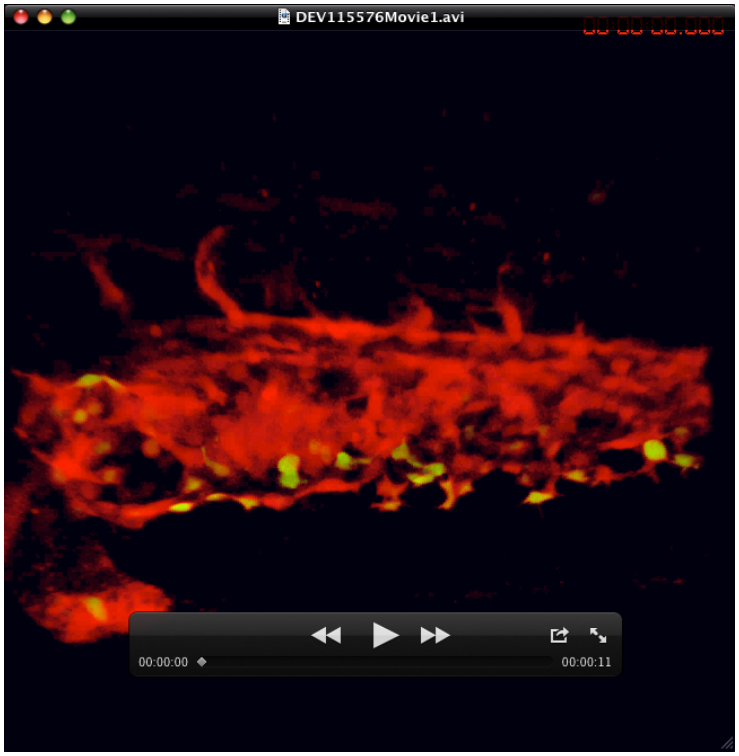

Supplementary Movie 1. β-catenin-mediated gene expression is induced in the ECs that sprout from CV primordia. Time-lapse confocal imaging of the CV formation in the *Tg(fli1:Gal4db-TΔC-2A-mC);(UAS:GFP);(fli1:Myr-mC)* embryo. Green, GFP fluorescence (β-Cat activity); red, mCherry fluorescence (ECs). The recording started at 24 hpf. Elapsed time (hr:min:sec:msec).

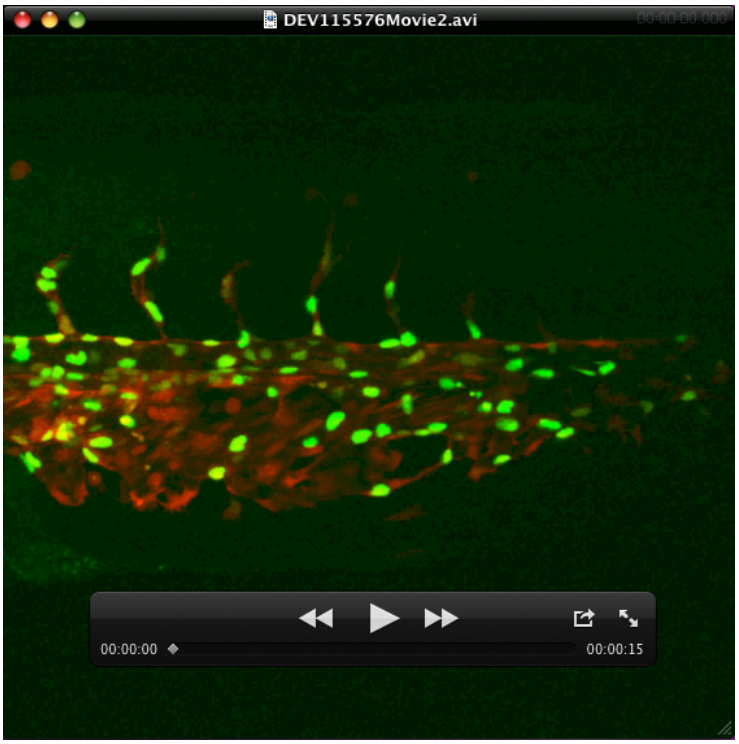

Supplementary Movie 2. Inhibition of β-catenin/Tcf-dependent transcription results in nuclear fragmentation of the ECs in the CVP, but not in the caudal artery. Time-lapse confocal imaging of the CV formation in the *Tg(fli1:Gal4FF);(UAS:RFP);(UAS:TΔN-GFP)* embryo. Green, GFP fluorescence (TΔN-GFP-expressing ECs); red, mCherry fluorescence (ECs). The recording started at 30 hpf. Elapsed time (hr:min:sec:msec).

References

Aranguren, X. L., Beerens, M., Vandevelde, W., Dewerchin, M., Carmeliet, P. and Luttun, A. (2011). Transcription factor COUP-TFII is indispensable for venous and lymphatic development in zebrafish and Xenopus laevis. *Biochem. Biophys. Res. Commun.* **410**, 121-126.

Asakawa, K., Suster, M. L., Mizusawa, K., Nagayoshi, S., Kotani, T., Urasaki, A., Kishimoto, Y., Hibi, M. and Kawakami, K. (2008). Genetic dissection of neural circuits by Tol2 transposon-mediated Gal4 gene and enhancer trapping in zebrafish. *Proc. Natl. Acad. Sci. USA* **105**, 1255-1260.

Bussmann, J., Bos, F. L., Urasaki, A., Kawakami, K., Duckers, H. J. and Schulte-Merker, S. (2010). Arteries provide essential guidance cues for lymphatic endothelial cells in the zebrafish trunk. *Development* **137**, 2653-2657.

Chen, D., Li, L., Tu, X., Yin, Z. and Wang, Q. (2013). Functional characterization of Klippel-Trenaunay syndrome gene AGGF1 identifies a novel angiogenic signaling pathway for specification of vein differentiation and angiogenesis during embryogenesis. *Hum. Mol. Genet.* **22**, 963-976.

Chung, J. H., Whiteley, M. and Felsenfeld, G. (1993). A 5' element of the chicken beta-globin domain serves as an insulator in human erythroid cells and protects against position effect in Drosophila. *Cell* **74**, 505-514.

Fukuhara, S., Sako, K., Minami, T., Noda, K., Kim, H. Z., Kodama, T., Shibuya, M., Takakura, N., Koh, G. Y. and Mochizuki, N. (2008). Differential function of Tie2 at cell-cell contacts and cell-substratum contacts regulated by angiopoietin-1. *Nat. Cell Biol.* **10**, 513-526.

Halloran, M. C., Sato-Maeda, M., Warren, J. T., Su, F., Lele, Z., Krone, P. H., Kuwada, J. Y. and Shoji, W. (2000). Laser-induced gene expression in specific cells of transgenic zebrafish. *Development* **127**, 1953-1960.

Kawakami, K., Takeda, H., Kawakami, N., Kobayashi, M., Matsuda, N. and Mishina, M. (2004). A transposon-mediated gene trap approach identifies developmentally regulated genes in zebrafish. *Dev. Cell* **7**, 133-144.

Lawson, N. D. and Weinstein, B. M. (2002). In vivo imaging of embryonic vascular development using transgenic zebrafish. *Dev. Biol.* **248**, 307-318.

Robu, M. E., Larson, D. J., Nasevicius, A., Beiraghi, S., Brenner, C., Farber, S. A. and Ekker, S. C. (2007). p53 activation by knockdown technologies. *PLoS Genet.* **3**, e78.

Totong, R., Schell, T., Lescroart, F., Ryckebüsch, L., Lin, Y. F., Zygmunt, T., Herwig, L., Krudewig, A., Gershoony, D., Belting, H. G. et al. (2011). The novel transmembrane protein Tmem2 is essential for coordination of myocardial and endocardial morphogenesis. *Development* **138**, 4199-4205.

Urasaki, A., Morvan, G. and Kawakami, K. (2006). Functional dissection of the Tol2 transposable element identified the minimal cis-sequence and a highly repetitive sequence in the subterminal region essential for transposition. *Genetics* **174**, 639-649.

Zhang, J., Fukuhara, S., Sako, K., Takenouchi, T., Kitani, H., Kume, T., Koh, G. Y. and Mochizuki, N. (2011). Angiopoietin-1/Tie2 signal augments basal Notch signal controlling vascular quiescence by inducing delta-like 4 expression through AKT-mediated activation of β-catenin. *J. Biol. Chem.* **286**, 8055-8066.

Zygmunt, T., Gay, C. M., Blondelle, J., Singh, M. K., Flaherty, K. M., Means, P. C., Herwig, L., Krudewig, A., Belting, H. G., Affolter, M. et al. (2011). Semaphorin-PlexinD1 signaling limits angiogenic potential via the VEGF decoy receptor sFlt1. *Dev. Cell* **21**, 301-314.